NIH Public Access
Author Manuscript
Motor Control. Author manuscript; available in PMC 2010 July 1.

Published in final edited form as:
Motor Control. 2009 July ; 13(3): 251–279.

Mechanical Analysis and Hierarchies of Multi-digit Synergies during Accurate Object Rotation

Wei Zhang, **Halla B. Olafsdottir**, **Vladimir M. Zatsiorsky**, and **Mark L. Latash**
Department of Kinesiology, The Pennsylvania State University, University Park, PA 16802

Abstract

We studied the mechanical variables (the grip force and the total moment of force) and multi-digit synergies at two levels (the virtual finger-thumb level, VF-TH, and the individual finger level, IMRL) of a hypothetical control hierarchy during accurate rotation of a hand-held instrumented handle. Synergies were defined as co-varied changes in elemental variables (forces and moments of force) that stabilize the output at a particular level. Indices of multi-digit synergies showed higher values at the hierarchically higher level (VF-TH) for both normal and tangential forces. The moment of force was stabilized at both hierarchical levels during the steady-state phases but not during the movement. The results support the principles of superposition and of mechanical advantage. They also support an earlier hypothesis on an inherent trade-off between synergies at the two hierarchical levels, although the controller showed more subtle and versatile synergic control than the one hypothesized earlier.

Keywords

prehension; synergy; hierarchical control; hand; principle of superposition

Introduction

Control hierarchies for human movements have been invoked for at least half a century (Bernstein, 1947, 1967, 1996; Arbib, Iberall, & Lyons, 1985). In particular, the multi-digit actions during human prehensile tasks have been viewed as produced by a control hierarchy involving two levels: the virtual finger-thumb level (VF-TH) and the individual finger level (IMRL, index-middle-ring-little level). The virtual finger (VF) is an imagined digit that produces a mechanical action equivalent to that of the actual fingers of the hand (Arbib et al., 1985; Mackenzie & Iberall, 1994a). Synergies, defined as conjoint changes in mechanical outputs of individual digits stabilizing their overall action (Latash, Scholz, & Schoner, 2007; Zatsiorsky & Latash, 2004), have been assumed to exist at both levels of the hierarchy. At the upper level, synergic action of the VF and thumb stabilizes the total force and/or the total moment of force produced on the hand-held object. At the lower level, synergic action of the individual fingers stabilizes the output of the VF.

Several studies investigated the force and moment of force production tasks during pressing, grasping, and holding an object (Baud-Bovy & Soechting, 2001; Gao, Latash, & Zatsiorsky, 2005; Pataky, Latash, & Zatsiorsky, 2004a, b; Santello & Soechting, 2000; Shim, Latash, & Zatsiorsky, 2005a, b; Zatsiorsky, Gao, & Latash, 2003a). Multi-digit synergies during prehensile tasks have been shown to stabilize the force magnitude, point of force application,

Address for correspondence: Mark Latash, Department of Kinesiology, Rec.Hall-268N, Penn State University, University Park, PA 16802, USA, Email: mll11@psu.edu, Tel: (814) 863-5374.

NIH-PA Author Manuscript
NIH-PA Author Manuscript
NIH-PA Author Manuscript

NIH-PA Author Manuscript

NIH-PA Author Manuscript

NIH-PA Author Manuscript

and direction of the VF force by the co-variation among the outputs of the individual fingers (Gao et al., 2005; Latash, Li, Danion, & Zatsiorsky, 2002b), while the coordinated action of the VF and the thumb stabilized the gripping and rotational action components on the hand-held object (Shim et al., 2005a; Zatsiorsky et al., 2003a). These findings suggest co-existence of synergies at the two hierarchical levels.

However, recent studies of multi-finger pressing (Gorniak, Zatsiorsky, & Latash, 2007a, b; Kang, Shinohara, Zatsiorsky, & Latash, 2004) have suggested that the central nervous system (CNS) may face problems with organizing force stabilizing synergies at two levels of a control hierarchy simultaneously. In those studies, negative co-variation between the finger forces was observed within two- and four-finger groups within-a-hand in the one-hand force-production tasks. Such co-variation apparently reduced the variability of the total force. However, no negative co-variation was seen between fingers of a hand in the two-hand tasks, while the total forces produced by each hand did co-vary negatively in those tasks. These results have been interpreted as reflecting an inherent trade-off between synergies at the two levels of a control hierarchy (Gorniak et al., 2007b).

Until now, most studies of multi-finger synergies focused on constrained pressing tasks or static prehensile tasks. Everyday actions involving manipulation of hand-held objects, such as drinking from the glass, eating with the spoon, handwriting, etc. typically require precise time patterns of the resultant moment of force that have to be accompanied by adequate adjustments of the grip force. Since grip force, resultant force, and resultant moment of force depend on the same elemental variables (force vectors produced by the digits), the task of ensuring their coordinated changes in a task-specific way requires nontrivial coordinated changes of the elemental variables. Note that accurate rotational actions are of particular importance for everyday tasks: An error in the total moment of force may lead to spilling the contents of the glass while the grip force may range broadly as long as it does not lead to dropping or crushing the object. Besides its obvious practical importance, the issue of digit coordination in natural tasks has important implications for the issue of constraints on digit coordination that may be imposed by the mentioned inherent trade-off between synergies at different levels of a multi-level control hierarchy.

Only a few studies investigated digit coordination during more natural prehensile hand actions in 3D space (Gao et al., 2005; Bursztyn & Flanagan, 2008; Winges, Eonta, Soechting, & Flanders, 2008). In particular, a recent study addressed finger coordination during object rotation grasped with three digits (Winges et al., 2008). This study used principal component analysis of electromyographic and force signals and reported two main temporal patterns associated with position and velocity of the object.

In the current study, we used a prismatic grasp involving all five digits of the dominant hand and examined the multi-digit synergies during accurate three-dimensional rotational hand actions (similar to taking a sip from the glass) in an attempt to: 1) explore the preferred solutions at the two levels, VF-TH and IMRL; 2) explore the variance structure of the mechanical variables produced by the digits (elemental variables) with respect to stabilization of the total force and moment of force (performance variables); 3) examine the interference between force and moment-of-force stabilizing synergies at the two hierarchical levels. Based on the mentioned studies by Gorniak et al. (2007a, b), we hypothesized that force and moment-of-force stabilizing synergies would be observed at the VF-TH level, while they might be absent at the IMRL level.

NIH-PA Author Manuscript

NIH-PA Author Manuscript

NIH-PA Author Manuscript

Methods

Subjects

Nine (five males and four females) healthy young volunteers participated in this study (age: 27.3 ± 1.2 yr, mean ± SE). All participants (weight: 63.5 ± 2.9 kg; height: 1.71 ± 0.024 m) were right-handed according to their preferred hand use for writing and eating. The right hand width measured at the metacarpophalangeal joint level averaged as 0.086 ± 0.001m for males and as 0.073 ± 0.002m for females; the right hand length measured from the midpoint of the transverse wrist crease to the tip of the middle finger was 0.18 ± 0.002m for male and 0.17 ± 0.003m for female subjects. All participants gave informed consent according to the procedures approved by the Office for Research Protection of the Pennsylvania State University.

Apparatus

The experiment setup is illustrated in Figure 1. There were five six-component force/moment transducers, one NANO-25 sensor for the thumb and four NANO-17 sensors for the four fingers. The sensors measured three force and three moment-of-force components produced by the individual digits in the local coordinate systems of the transducers. The transducers for the thumb (TH) and for the four fingers (I - Index; M -Middle; R - Ring; and L - Little) were mounted on opposite sides of a PVC (Polyvinyl chloride) vertical handle. The sensors were attached to the handle in such a way that the Y axes of all sensors were parallel to the central vertical axis of the handle. The center of the sensor base for TH was aligned along the central frontal axis of the handle. The geometric dimensions of the sensors and handle are shown in Figure 1C.

To increase the friction between the digits and the contact surfaces, the surface of each sensor was covered with 100-grit sandpaper (static friction coefficients between the digit tip and the contact surface ranged from 1.4 to 1.5, (Zatsiorsky, Gregory, & Latash, 2002). The thirty analogue force/moment output signals from the sensors were digitalized at 12 bits (PCI-6225, National Instrument, Austin, TX, USA). The force and moment of force measured by each sensor were sampled at 200 Hz, with a 12-bit resolution by a PC computer (Dell Optiplex GX620) and processed by a customized LabView-based (Labview 8.0, National Instrument, Austin, TX, USA) program.

Two inertial loads (copper cylinders, 0.1 kg each) were attached along a diameter of a PVC disc (25 cm in diameter), 9.5 cm away from the center of the disc. The disc was connected to the handle by a 19-cm aluminum rod, which was attached through the geometrical centers of both the disc and handle, perpendicular to their vertical axes (Figure 1B). The disc, rod and handle (DRH) formed a rigid body that could be rotated as a single piece about the long axis of the rod. Two levels were attached to the top of the DRH system to detect its tilting in the sagittal and frontal planes. Both levels were placed horizontally with one parallel to the rod and the other one orthogonal to the rod (Figure 1B). The weight of the DRH system was balanced by a counter-load (0.76 kg) that was hooked by a rock climbing rope through a couple of pulleys fixed to the ceiling. During the experiment, the DRH could be rotated freely about the horizontal axis coinciding with the rod (the friction between the rod and the ring was very small), while the subject did not have to counteract the weight of the DRH system that was balanced in both frontal and sagittal planes.

During the test, the subject sat comfortably in the height-adjustable chair facing the testing device (Figure 1A). His/her right forearm was placed into a PVC forearm brace that was fixed to a small table. A sponge pad was used between the forearm and the brace to increase comfort. A single-axis torsiometer (Biometrics Ltd, Gwent, UK) was attached to measure hand pronation-supination (PR-SU) angle (A_W). To attach the torsiometer, the subject was instructed

NIH-PA Author Manuscript

NIH-PA Author Manuscript

NIH-PA Author Manuscript

to fully extend the wrist and hand joints with the palm down on the table. The two end pieces of the torsiometer were attached to the midline of the hand dorsal surface and to the middle of the forearm. A pair of Velcro straps was used to keep the forearm from moving in flexion-extension and adduction-abduction. The right upper arm was at about 45° of flexion in the sagittal plane and the forearm was at about 90° of pronation when the subject grasped the handle in its vertical orientation. The distal edge of the brace was aligned with the transverse wrist crease so that the subject could rotate the hand freely in the frontal plane. A 17-in liquid crystal display monitor, placed about 1 m in front of the subject, displayed both the task (the initial and target handle orientations) and the current subject's PR-SU angle (A_W) recorded by the torsiometer.

Procedure

Before each trial, the handle was oriented vertically and the sensor signals were set to zero in the absence of digit forces such that only signal deviations produced by the subject were recorded and analyzed. Zero position of the torsiometer was defined as the orientation when the two end pieces were put flat on a plane. There was a non-zero initial A_W for each subject due to the natural differences in the initial wrist position. Therefore, each subject performed one self-calibration trial before the main experimental tasks. During the self-calibration trial, the subject was asked to grasp the handle in his/her most comfortable position while keeping the two levels horizontal. This position was held for 10 s, and the averaged A_W was computed across that time interval and used to set the following tasks. This procedure allowed setting visual feedback on A_W to zero at the initial position for all the subjects. The most comfortable position was defined as the neutral (NE) position. Consequently, pronation (PR) and supination (SU) were defined with respect to the NE position rather than to the anatomically neutral position.

The main tasks required the subjects to produce a quick rotation from an initial to a target position at one of the two speeds, natural (slow, SL) and as fast as possible (fast, FA) in both PR and SU. The screen always showed the subject two thick yellow lines corresponding to 30° positive (SU) and negative (PR) A_W with respect to NE. These lines worked as the initial and target positions. There were two horizontal dashed thin lines above and bellow each of the two thick lines to show the subject the allowable error range (±5°) during the tasks. A line in-between the two yellow lines corresponded to the NE position. Two vertical dashed thin lines served as event reminders, with the first one 1.5 s from the trial initiation (it reminded the subject to start rotating from the NE position to the initial position at a self-selected speed) and the second one 5 s after the trial initiation (it reminded the subject to produce a rotation from the starting to the target position; Figure1A).

There were four task conditions, PR-FA; PR-SL; SU-SL; and SU-FA. During each trial, the subject first kept the NE position for 1.5 s. Then, the subject rotated the handle from the NE position into the initial position and held this position as accurately as possible for at least 1.5 s. Note that there was no speed or accuracy requirement for the subject during that preparatory motion. Further, the subject produced a voluntary rotation at the instructed speed and in the instructed direction to the target position. During the rotation, the subject was instructed to produce a smooth motion into the target area and not to correct the final position even if it happened to be inaccurate. As long as the subject stopped within the error range, the data were accepted. Inaccurate trials were rejected immediately and repeated (there were no more than 5 repeated trials per condition for each subject).

Five practice trials were given prior to each condition. For each condition, twenty-four consecutive trials were collected with 8-s time intervals between trials. The conditions were presented in a balanced order. There were 2-min rest period between conditions.

NIH-PA Author Manuscript

NIH-PA Author Manuscript

NIH-PA Author Manuscript

Initial data processing

Data processing was performed off-line using MATLAB 7.0, Excel, and Minitab software. Signals starting from 0.5 s prior to the movement initiation and ending 2 s after the movement termination were used for analysis. The angular velocity ($\dot{A}_w$) was calculated for each trial. The initiation and termination of movement were respectively defined as the instances when $\dot{A}_w$ reached 5% of its peak value and when it first dropped below 5% of its maximal value in each trial. All trials were aligned by the movement onset. Since individual rotations differed in their duration, the trials were time normalized to 100% and the data were re-sampled to 100 points over the trial duration. This time normalization was only performed over the movement duration, but not for the time intervals before and after the movement. Specifically, in the following sections and illustrations, the times of onset and ending of the movement would be referred to as negative zero (−0) and positive zero (+0) respectively, and time prior to the movement and after the movement will be presented as negative and positive values in seconds with respect to the onset or end of movement. For instance, one second before the movement onset is referred to as −1 s, and one second after the movement termination is referred to as +1 s.

Because each digit makes a soft-finger contact with the sensor surface (Arimoto, Nguyen, Han, & Doulgeri, 2000; Mason & Salisbury, 1985; Shim, Latash, & Zatsiorsky, 2003), the digit tips can roll on the sensors. Digits could push against the sensors but could not pull on them. The coordinates of the point of digit force application with respect to the center of the surface of the sensor along y axis was calculated as: $\mathrm{COP}^{\mathrm{Y}} = \frac{Mx}{Fz}$ (Zatsiorsky, 2002), where COP stands for the center of pressure on the sensor surface; *Mx* stands for the moments about x axis; *Fx*, *Fy*, and *Fz* signify the force along x, y and z axis separately. The moments of force acting on the handle were calculated with respect to the longitudinal axis of the rod, whose x and y coordinates coincided with the center of thumb sensor.

The data were analyzed at two levels: the individual finger (IMRL) and the virtual finger-thumb (VF-TH) level. The VF is an abstract representation of the four individual fingers; the VF produces the same mechanical effects as all the individual finger forces and moments combined (Arbib et al., 1985; Baud-Bovy & Soechting, 2001; Cutkosky & Howe, 1990; Mackenzie & Iberall, 1994b; Shim, Latash, & Zatsiorsky, 2004). In other words, VF force is the vector sum of all individual finger forces (Eq. 1) and VF moment is the vector sum of moments produced by the fingers (Eq. 2).

$$F_{VF} = [F_{VF}^X, F_{VF}^Y, F_{VF}^Z]^T = [\sum_{i=1}^{4} F_i^X + \sum_{i=1}^{4} F_i^Y + \sum_{i=1}^{4} F_i^Z]^T \quad (1)$$

$$M_{VF} = [M_{VF}^X, M_{VF}^Y, M_{VF}^Z]^T = [\sum_{i=1}^{4} F_i^X d_i^X + \sum_{i=1}^{4} F_i^Y d_i^Y + \sum_{i=1}^{4} F_i^Z d_i^Z]^T \quad (2)$$

Antagonist moments of force

Due to the way moment of force was calculated, the normal forces produced by two pairs of fingers (IM and RL) acted as opponents since IM normal force always produced moment of force into PR and RL normal force always contributed to SU. This means that, at any time, one of the finger pairs produced moment of force against the direction of the total moment of force.

NIH-PA Author Manuscript

NIH-PA Author Manuscript

NIH-PA Author Manuscript

We defined *Agonist Moment* (M_{AGO}) as the moment produced in the direction of the total moment of force and *Antagonist Moment* (M_{ANT}) as the moment opposing the total moment of force. The role of the two finger pairs switched when subjects changed the resultant moment of force direction during the task. We used a co-contraction index of VF (Co_I_{VF}) calculated as the quotient of M_{ANT} with respect to M_{AGO}:

$$Co\_I_{VF} = \frac{M_{ANT}}{M_{AGO}} = \frac{Min(|M_{IM}|, |M_{RL}|)}{Max(|M_{IM}|, |M_{RL}|)}.$$

In addition, because the point of application of the thumb normal force could displace up or down with respect to the sensor center, the thumb force could also generate a moment with respect to the rod axis. The TH moment of normal force could contribute to the total moment of force or act against it as. To quantify the contribution of TH to the antagonist moment, we used an index of TH coactivation, Co_I_{TH}, computed as the percentage time when the force produced by TH contributed to M_{ANT} within a given time window. The Co_I_{TH} index was calculated as: $Co\_I_{TH} = \frac{T_{MANT}}{T_{TOT}} \times 100\%$, where T_{MANT} refers to the duration of time when the force of TH contributed to M_{ANT}; while T_{TOT} refers to the total time of interest.

Finger sharing pattern

Finger normal force sharing was defined as the percentages of normal force produced by the individual fingers (SF_i^N, i= I,M,R,L) to the normal force of VF. SF_i^N was computed for each time sample and then averaged across 24 trials in each condition for each subject.

An index of synergy

To analyze how the fingers interacted with each other and quantify the multi-finger synergies, we followed the variance analysis formulated in an earlier study (Latash, Kang, & Patterson, 2002a). An index (ΔV) of a synergy formed by a set of elements was calculated as the difference between the sum of the variances of individual element outputs and the variance of the overall output of the system, both computed over the 24 trials at each task performed by each subject. Note that for non-correlated random variables, the sum of the variances should be equal to the variance of the sum (the Bienaime equality). Variance analysis was performed at the two hierarchical levels, the VF-TH level and the individual finger level (IMRL). The ΔV index was calculated for several performance variables, which are the left-hand side variables in the following equations:

At the VF-TH level:

$$F^N = F^N_{VF} + F^N_{TH} \quad (3)$$

$$F^T = F^T_{VF} + F^T_{TH} \quad (4)$$

$$M_{TOT} = M^N_{VF} + M^N_{TH} + M^T_{VF} + M^T_{TH} \quad (5)$$

At the IMRL level:

NIH-PA Author Manuscript

NIH-PA Author Manuscript

NIH-PA Author Manuscript

$$F_{VF}^{N}=F_{I}^{N}+F_{M}^{N}+F_{R}^{N}+F_{L}^{N} \quad (6)$$

$$F_{VF}^{T}=F_{I}^{T}+F_{M}^{T}+F_{R}^{T}+F_{L}^{T} \quad (7)$$

$$M_{VF}^{N}=M_{I}^{N}+M_{M}^{N}+M_{R}^{N}+M_{L}^{N} \quad (8)$$

$$M_{VF}^{T}=M_{I}^{T}+M_{M}^{T}+M_{R}^{T}+M_{L}^{T} \quad (9)$$

$$M_{VF}=M_{I}^{N}+M_{M}^{N}+M_{R}^{N}+M_{L}^{N}+M_{I}^{T}+M_{M}^{T}+M_{R}^{T}+M_{L}^{T} \quad (10)$$

where subscript at the force variables (*F*) and moment of force variables (*M*) refer to the digits; *TOT* relates to the resultant moment of force produced by all five digits including the thumb. Superscripts in the above equations refer to the normal force (N) or tangential force (T). Please note that all the moment of force calculations refer to the moments produced around the logitudinal axis of the rod corresponding to the axis of instructed rotation.

To describe the calculation of the synergy index (ΔV), consider Eq. (3) above as an example. To remind, the raw time profiles were aligned by the onset of the handle rotation and the rotation duration was normalized to 100%. Variances were calculated for each 1% of the movement duration and for each time sample for the time intervals prior to the initiation and after the termination of each movement. The computation was performed over 24 trials for each condition and each subject separately. To examine the existence of a synergy between the normal forces produced by the VF (F_{VF}^{N}) and by the TH (F_{TH}^{N}), time profiles of the variance of the VF normal force ($Var(F_{VF}^{N})$), of the TH normal force ($Var(F_{TH}^{N})$) and of the total normal force ($Var(F^{N})$) were computed over trials. The time profile of the sum of variances of the VF and TH normal forces was also computed: $\sum Var(F_{VF,TH}^{N})=Var(F_{VF}^{N})+Var(F_{TH}^{N})$. Further, comparison was performed between the sum of variances and variance of the sum to assess the predominance of positive or negative co-variation of the normal forces produced by VF and TH. The index was normalized by $\sum Var(F_{VF,TH}^{N})$ for comparisons across conditions and subjects: $\Delta V\_F_{VF,TH}^{N}=\frac{\sum Var(F_{VF;TH}^{N})-Var(F^{N})}{\sum Var(F_{VF;TH}^{N})}$.

Positive values of ΔV ($\Delta V>0$) indicate predominantly negative co-variation between the VF and TH forces, and may be interpreted as a synergy stabilizing the resultant normal force with respect to its average value across the trials. In contrast, $\Delta V<0$ indicates predominantly positive co-variations between the VF and TH force, which can be seen as destabilizing the total normal force at the VF-TH level (Scholz, Kang, Patterson, & Latash, 2003). Such computations were performed for each of the equations (3) – (10).

NIH-PA Author Manuscript

NIH-PA Author Manuscript

NIH-PA Author Manuscript

Statistical analysis

Standard methods of parametric statistics were used; data are presented as means and standard errors. Mixed-effects analysis of variance (ANOVA) was used to analyze a variety of indices such as sharing, antagonist moment, COP coordinates of the resultant force and synergy indices (ΔV) with factors including *Peak (*two levels, PR_{MAX}, SU_{MAX}*)*, *Contributor* (four levels; M^{N}_{VF}, M^{N}_{TH}, M^{T}_{VF} *and* M^{T}_{TH}), *Speed* (two levels; *SL, FA)*, *Direction* (two levels; *PR, SU*), *Time-Interval* (four or five levels; *PRE, POST, T_PRMAX, T_ SUMAX, T_M0*), *Finger* (four levels; *I, M, R, L*), *Position* (two levels; *PPR* and *PSU*), *Variable* (three levels; COP^{Y}_{VF}, COP^{Y}_{TH}, $dCOP^{Y}$), and *Index* (two levels; $\Delta V\_M^{N}_{1MRL}$, $\Delta V\_M^{N+T}_{1MRL}$). Please note that the factor of *Position* refers to the pronation and supination positions independently of whether those served as initial or final positions. Factors for particular comparisons will be introduced in more detail later in the Results session. Data expressed in percent (sharing of finger force, indices of antagonist moment) were subjected to Fisher's z-transformation before using parametric methods of analysis. Since ΔV indices are limited by +1, their positive values were transformed as follows before further statistical analyses: $\Delta V = 0.5[\ln(1+\Delta V) - \ln(1-\Delta V)]$. Tukey's honestly significant difference (HSD) tests and pair-wise contrasts were applied to further explore significant effects.

Results

This section is organized in the following way. First, analysis of different mechanical variables is presented, followed by analysis of multi-digit synergies. We describe in detail only the results of ANOVAs that are later addressed in the Discussion. The *Speed* factor had significant main effects on several performance variables such as resultant moment of force and grip force. We will not describe these effects of *Speed* since most of them follow straightforward mechanics.

Mechanical analysis

Performance of the task—For all tasks, an ideal performance would correspond to rotation amplitude of 60°, starting from 30° SU/PR and stopping at 30° PR/SU. Figure 2 shows the averaged across 24 trials trajectories for a typical subject with standard error bars. Note that the time axis prior to movement initiation (PRE) and after the movement termination (POS) is in seconds, while movement time is normalized to 100%. The data are shown for the two fast conditions (PR-FA in panel A and SU-FA in panel B). Note the overall accurate performance of the task. Figure 1C displays the averaged across trials time profiles of the resultant moment of force produced by all digits in the plane of rotation (M_{TOT}) and grip force (F_{GRIP}; calculated as the normal force produced by the TH) for the same subject under the PR-FA condition. To remind, the moment of force was calculated with respect to the axis of rotation coinciding with the longitudinal axis of the rod (see Method). M_{TOT} was close to zero during the PRE and POS phases, while during the movement it showed two prominent peaks into PR (PR_{MAX}; 0.373 Nm) and into SU (SU_{MAX}; −0.282 Nm). F_{GRIP} was rather low prior to the movement (3.2 N); we would like to remind that the weight of the system was counterbalanced, so that the subjects did not have to act against gravity. F_{GRIP} showed a quick increase to over 11 N during the rotation, and dropped to a somewhat higher steady-state level (5.35 N) after the movement. Note also the two peaks of F_{GRIP} (11.1 N and 11.4 N), timed close to the M_{TOT} peaks, with a valley in-between. Such peak couples were seen clearly in only seven out from nine subjects in different conditions.

The averaged performance variables across subjects with standard errors under the four conditions are presented in Table 1. In additional to F_{GRIP}, movement amplitude (Amplitude of Aw), movement time (time of ROT), and peak values of the total moment of force, M_{TOT} into PR and SU directions are presented.

NIH-PA Author Manuscript

NIH-PA Author Manuscript

NIH-PA Author Manuscript

Subjects gripped the handle with lower forces during the steady-states (PRE and POS) with a transient grip force increase during the rotation. Specifically, the average F_{GRIP} during PRE and POS was lower than F_{GRIP} quantified at certain critical time points during the movement when M_{TOT} reached its peaks into PR (T_PR_{MAX}) and into SU (T_SU_{MAX}) and when M_{TOT} was zero (T_M_0) (Table 1). These observations have been confirmed by a three-way ANOVA with factors: *Time (PRE, POST, T_PR_{MAX}, T_SU_{MAX}, T_M_0)* × *Speed (SL, FA)* × *Direction (PR, SU)*. There was a main effect of *Time* ($F_{[4, 164]} = 4.92$; $p < 0.005$). Post-hoc Tukey's tests indicated that F_{GRIP} during PRE had lower values than those during the movement (T_PR_{MAX}, $p<0.005$; T_SU_{MAX}, $p<0.01$; T_M0, $p<0.05$).

Sharing of mechanical variables—The resultant moment of force (M_{TOT}) can be decomposed into four contributors at the VF-TH level (Mi_VF-TH): moments produced by the normal forces of VF (M^N_{VF}) and TH (M^N_{TH}), and moments produced by the tangential forces of VF (M^T_{VF}) and TH (M^T_{TH}). Figure 3 shows the average time profiles of M_{TOT} and the four contributors under the four conditions (A: PR-SL; B: PR-FA; C: SU-SL; and D: SU-FA). Generally, the four moment contributors showed time profiles similar to that of M_{TOT}. Please note that the two lines representing the moments produced by the tangential forces of VF and TH overlap under all conditions. This result follows straightforward mechanics, given the fact that the lever arms of the tangential forces of VF and TH were the same and that the tangential forces had similar magnitudes to avoid translational motion of the handle.

Figure 3 indicates that moment produced by the normal force of VF (M^N_{VF}) was the most dominant contributor to M_{TOT} during the movement. When M_{TOT} reached its PR_{MAX} (T_PR_{MAX}), M^N_{VF} contributed more than 50% and 40% to M under the SL and FA conditions, respectively. At T_SU_{MAX}, the four contributors showed different amplitudes but similar time profiles. These observations have been confirmed by a three-way ANOVA on Mi_VF-TH at T_PR_{MAX}, *Contributor* (M^N_{VF}, M^N_{TH}, M^T_{VF} *and* M^T_{TH}) × *Speed (SL, FA)* × *Direction (PR, SU)*. *Contributor* showed a main effect ($F_{[3, 131]} = 12.74$; $p < 0.001$). Post-hoc Tukey's tests indicated that M^N_{VF} at T_PR_{MAX} was significantly higher than the other three M_{TOT} contributors (M^N_{TH}, M^T_{VF} *and* M^T_{TH}), $p<0.001$.

At the individual finger level (IMRL), moment of force produced by VF was shared by four components (Mi_IMRL) produced by the I (M_I), M (M_M), R (M_R) and L (M_L) fingers. Figure 4 shows the finger moment of force time profiles under the four conditions (A: PR-SL; B: PR-FA; C: SU-SL; and D: SU-FA). M_I and M_M are positive and add up to the PR moment produced by VF, while the other two fingers (R and L) produce SU moment shown as negative values. Under all four conditions, I and L dominated the PR and SU moment production, respectively, as compared to M and R. The larger moments of force produced by I and L have been confirmed by a four-way ANOVA on Mi_IMRL: *Finger (I, M, R, L)* × *Time-Interval (PRE, POST, T_PR_{MAX}, T_SU_{MAX})* × *Speed (SL, FA)* × *Direction (PR, SU)*. *Finger* showed a main effect ($F_{[3, 581]} = 252.36$; $p < 0.001$). Post-hoc Tukey's tests indicated that moments produced by individual fingers were significantly different from each other: $M_I > M_M > M_R > M_L$, $p<0.0001$. There was also a main effect of *Time-Interval* ($F_{[3, 581]} = 31.14$; $p < 0.001$). Post-hoc Tukey's tests showed that moment of force at T_PR_{MAX} was higher than at PRE and POS, which were higher than those at T_SU_{MAX}, $p<0.0005$. Besides, there was a *Finger* × *Time-Interval* interaction ($F_{[9, 581]} = 10.96$; $p < 0.001$), whereas there was no main effect of *Speed* and *Direction*.

Figure 5 shows the average sharing patterns of the normal force across the individual fingers (SF^N_I, SF^N_M, SF^N_R, SF^N_L) under the four conditions (A: PR-SL; B: PR-FA; C: SU-SL; and D: SU-

NIH-PA Author Manuscript

NIH-PA Author Manuscript

NIH-PA Author Manuscript

FA). The sharing patterns were relatively stable during the PRE and POS phases. SF^N_I and SF^N_M contributed more than 50% of the VF normal force during PRE and POS across all conditions with the largest share of I. Finger normal force sharing varied substantially during the movement, especially for the fingers (I and L) with longer lever arms. SF^N_I and SF^N_L showed opposite changes under all conditions with larger variations in FA (25% for I and 15% for L) than in SL (15% for I and 10% for L) conditions.

Values of SF^N were transformed into Fisher's z-scores and subjected to a three-way ANOVA on the absolute difference between SF^N at T_PR_{MAX} and SF^N at T_SU_{MAX} with the factors *Finger (I, M, R, L)* × *Speed (SL, FA)* × *Direction (PR, SU)*. Both *Finger* and *Speed* showed main effects (*Finger*: $F_{[3, 131]} = 64.21$; $p < 0.001$; *Speed*: $F_{[1, 131]} = 16.36$; $p < 0.001$). Post-hoc Tukey's tests confirmed that the share changes for I and L fingers between the M_{TOT} peaks were significantly larger than for the other two fingers, $p<0.0001$. Besides, SF^N of each finger showed significantly larger changes under the FA conditions as compared to the SL conditions ($p<0.001$).

Antagonist moments produced by VF and TH—Antagonist (M_{ANT}) and agonist moments of force (M_{AGO}) have been defined as the moments that act in the opposite direction and in the same direction as the resultant moment (M_{TOT}) respectively. Two co-contraction indices were introduced to quantify M_{ANT} produced by VF and TH (see Methods). For VF, when I and M produced normal forces that generated M_{ANT}, R and L produced normal forces that generated M_{AGO}, and vice versa. We calculated a co-contraction index for VF (Co_I_{VF}) as the ratio of M_{ANT} to M_{AGO} produced by VF. Normal force of TH could produce M_{ANT} or M_{AGO} at different movement phases. Therefore, the co-contraction index of TH (Co_I_{TH}) was calculated as the percentage of time when TH produced M_{ANT} within a particular time interval. Three time intervals were considered: PRE (0.5 s duration), POS (0.5 s duration), and Rotation (100%).

Figure 6 shows the time profiles of averaged across subjects Co_I_{VF} under the four conditions (A: PR-SL; B: PR-FA; C: SU-SL; and D: SU-FA). Note that $Co\_ I_{VF}$ in PR conditions (PR-SL and PR-FA, thick lines) was larger during the PRE phase but smaller during the POS phase as compared to that in SU conditions (SU-SL and SU-FA, thin lines).

$Co\_ I_{VF}$ values during PRE and POS were transformed into Fisher's z-scores and subjected to a three-way ANOVA: *Position* (P_{PR}, P_{SU}) × *Speed* (*SL, FA*) × *Direction* (*PR, SU*). Only *Position* shows a main effect ($F_{[1, 66]} = 54.39$; $p < 0.001$) corresponding to higher $Co\_ I_{VF}$ when the handle was in the SU than in the PR position ($p<0.0001$). Furthermore, there was an interaction effect between *Position* and *Direction* ($F_{[1, 66]} = 5.95$; $p < 0.05$) with the switching of the *Position* levels for the SU tasks as compared to the PR tasks.

Table 2 shows the average values of Co_I_{TH} within these time intervals under the four conditions. Co_I_{TH} in the SU conditions showed larger values during PRE but smaller values during POS than Co_I_{TH} in PR conditions. Differences in Co_I_{TH} between these conditions were over 50%.

Co_I_{TH} values during PRE and POS were transformed into Fisher's z-scores and subjected to a three-way ANOVA: *Position* (P_{PR}, P_{SU}) × *Speed* (*SL, FA*) × *Direction* (*PR, SU*). Only *Position* showed a main effect ($F_{[1, 64]} = 64.20$; $p < 0.001$) reflecting higher values when the handle was in a PR position than in a SU position. There were no other main or interaction effects.

NIH-PA Author Manuscript

NIH-PA Author Manuscript

NIH-PA Author Manuscript

COP shifts for VF and TH—Due to the finger tip rolling over the sensor surface and changes in the individual finger force sharing pattern, the lever arm of the moment produced by the TH-VF normal force couple could change. The center of pressure of VF and TH (COP^Y_{VF} and COP^Y_{TH}) time profiles under the four conditions are displayed in Figure 7 (A: PR-SL; B: PR-FA; C: SU-SL; and D: SU-FA).

When the resultant normal forces were applied above the rod axis, COP^Y values were considered positive, whereas COP^Y values under the rod axis were considered negative. Please note that VF and TH applied normal force to the opposite sides of the handle, therefore a positive COP^Y would contribute to PR by VF but to SU by TH. Figure 7 shows that both COP^Y_{VF} and COP^Y_{TH} were kept at steady values during the PRE and POS phases, but they varied out-of-phase during the rotation. The variations of COP^Y were much larger than those of COP^Y under all the conditions, especially in the FA conditions, when the range of COP^Y was more than 2 cm.

A three-way ANOVA was performed on the absolute difference between the COP^Y values measured at T_PR_{MAX} and T_SU_{MAX} with factors: *Variable* (COP^Y_{VF}, COP^Y_{TH}) × *Speed (SL, FA)* × *Direction (PR, SU)*. There was a main effect of *Variable* ($F_{[2, 98]} = 116.93$; $p < 0.001$) with Tukey's post-hoc tests showing that changes in COP^Y_{VF} were significantly larger than those of COP^Y_{TH} ($p<0.0001$). There was also a main effect of *Speed* ($F_{[1, 98]} = 19.14$; $p < 0.001$) with significantly larger changes in the FA conditions for both variables from T_PR_{MAX} to T_SU_{MAX} than those in the SL conditions.

Synergy analysis

To recall, multi-digit synergies were quantified using an index (ΔV) calculated as the normalized difference between the sum of variances of elemental variables (produced by individual digits at the VF-TH or IMRL level) and variance of the overall output of all the digits at the selected level.

Synergies at the VF-TH level—To visualize the process of ΔV computation, we show the variance of force and moment of force components and variance of their sum at the VF-TH level in Figures 8, 10 and 11. Figure 8 shows the variance of M_{TOT} (V_M_{TOT}) and variances ($V\_M^N_{VF}$, $V\_M^T_{VF}$, $V\_M^N_{TH}$, $V\_M^T_{TH}$) of its four components (M^N_{VF}, M^T_{VF}, M^N_{TH}, M^T_{TH}) under the four conditions (A: PR-SL; B: PR-FA; C: SU-SL; and D: SU-FA). Under all the conditions, V_M_{TOT} (dash-dot line) shows much higher values over the movement time as compared to the other moment variances. The situation is opposite during the PRE and POS phases, when V_M_{TOT} shows the smallest values.

The ΔV indices computed for the total moment at the VF-TH level (ΔV_M_{VF-TH}) for the four conditions are displayed in Figure 9. Note the initially high positive values of ΔV_M_{VF-TH} (about + 0.66; note that +1 is the maximal possible value for ΔV). Then, these values dropped into negative values (on average, −0.92) over the movement time, and then increased back to relative high positive values (on average, +0.73) during the POS phase.

These observations have been confirmed by a three-way ANOVA on ΔV_M_{VF-TH} with factors: *Time (PRE, ROT, POS)* × *Speed (SL, FA)* × *Direction (PR, SU)*. There was a main effect of *Time* ($F_{[2, 98]} = 213.82$; $p < 0.001$). The post-hoc Tukey's tests showed that values of ΔV_M_{VF-TH} during both PRE and POS were significantly higher than those during ROT ($p<0.0001$). There were no other significant main or interaction effects.

NIH-PA Author Manuscript

NIH-PA Author Manuscript

NIH-PA Author Manuscript

Variances of the normal and tangential force components ($V\_F^N_{VF}$ and $V\_F^N_{TH}$, $V\_F^T_{VF}$ and $V\_F^T_{TH}$) and of their sums ($V\_F^N_{VF-TH}$, $V\_F^T_{VF-TH}$) are shown in Figures 10 and 11. Note the lower values of $V\_F^N_{VF-TH}$ and $V\_F^T_{VF-TH}$ (thin solid lines) as compared to the variances of the force components (thick solid and thick dash-dot lines). This was true over all the phases under all the conditions.

The average time profiles of ΔV indices for the normal ($\Delta V\_F^N_{VF-TH}$) and tangential force ($\Delta V\_F^T_{VF-TH}$) at the VF-TH level under all the conditions are presented in Figure 12A and B. Note that the ΔV indices are positive at all phases and under all four conditions; there are larger variations in $\Delta V\_F^T_{VF-TH}$ as compared to $\Delta V\_F^N_{VF-TH}$.

Synergies at the IMRL level—Figures 12C and D present results of the analysis of force co-variation (for the normal $\Delta V\_F^N_{IMRL}$, and tangential forces $\Delta V\_F^T_{IMRL}$) at the IMRL level. Please note the same span of the Y axes (equal to 1) in all the panels of Figure 12 but the different ranges of ΔV. Values of $\Delta V\_F^N_{IMRL}$ are negative over all the phases and under all four conditions, while $\Delta V\_F^T_{IMRL}$ shows positive values during PRE and POS and negative values over the movement duration under all conditions. Note that ΔV indices had higher values at the hierarchically higher level (VF-TH) than at the lower level (IMRL) for both normal and tangential force analysis (compare Figures 11 and 12).

These observations have been confirmed by a five-way ANOVA with factors: *Level (VF-TH, IMRL)* × *Force* (F^N, F^T) × *Time (PRE, ROT, POS)* × *Speed (SL, FA)* × *Direction (PR, SU)*. There was a main effect of *Level* ($F_{[1, 411]} = 2150.15$; $p < 0.001$) confirming significantly larger ΔV values at the VF-TH level than at the IMRL level. There was a main effect of *Force* ($F_{[1, 411]} = 73.96$; $p < 0.001$) corresponding to higher ΔV indices for F^T than for F^N ($p<0.0001$). Besides, there were an interaction effects *Level* × *Force* ($F_{[1, 411]} = 666.9$, $p < 0.001$), *Force* × *Duration* ($F_{[2, 411]} = 9.44$; $p < 0.001$), and *Level* × *Duration* ($F_{[2, 411]} = 3.95$; $p < 0.001$). Interaction plots for these effects confirmed that: 1) the difference between *Force* levels was higher for the IMRL level compared to the VF-TH level; 2) the difference between *Force* levels was higher for PRE and POS time intervals as compared to ROT; 3) the difference between *Level* levels was higher for ROT compared with PRE and POS.

At the IMRL level, synergy analysis was also performed for the moment produced by the normal force of VF (M^N_{VF}) and for the resultant moment produced by VF ($M^{N,T}_{VF}$) separately. Figure 13 displays the ΔV indices for M^N_{VF} ($\Delta V\_M^N_{IMRL}$; panel A) and $M^{N,T}_{VF}$ ($\Delta V\_M^{N,T}_{IMRL}$; panel B) under the four conditions. The ΔV patterns are similar, starting with positive values at PRE, dropping to zero or negative values over the movement time, and recovering to positive values during POS. Specifically, values of $\Delta V\_M^N_{IMRL}$ are smaller during PRE and POS but larger during the movement time than those of $\Delta V\_M^{N,T}_{IMRL}$.

These observations have been confirmed by a four-way ANOVA on the ΔV indices: *Index* ($\Delta V\_M^N_{IMRL}$, $\Delta V\_M^{N,T}_{IMRL}$) × *Time (PRE, ROT, POS)* × *Speed (SL, FA)* × *Direction (PR, SU)*. There was a main effect of *Time* ($F_{[2, 204]} = 175.71$; $p < 0.001$). The post-hoc Tukey's tests show that both ΔV indices ($\Delta V\_M^N_{IMRL}$, $\Delta V\_M^{N,T}_{IMRL}$) had larger values during PRE and POS than during ROT ($p<0.0001$). *Index* also showed a main effect ($F_{[1, 204]} = 9.4$; $p < 0.005$) with significantly higher values of $\Delta V\_M^{N,T}_{IMRL}$ ($p<0.005$). Besides, there were significant *Time* × *Index* ($F_{[2, 204]} = 35.89$; $p < 0.001$) and *Time* × *Direction* ($F_{[2, 204]} = 4.93$; $p < 0.005$) interactions, corresponding to larger values of $\Delta V\_M^N_{IMRL}$ during ROT but lower values during PRE and

NIH-PA Author Manuscript

NIH-PA Author Manuscript

NIH-PA Author Manuscript

POS as compared to $\Delta V\_M^{N,T}_{IMRL}$, and larger values of ΔV during PRE in PR conditions but lower values of ΔV during PRE in SU conditions compared to ΔV during POS.

Discussion

In the Introduction, we introduced a two-level control hierarchy (the upper VF-TH level and the lower IMRL level; Arbib et al. 1985) and hypothesized that force and moment of force stabilizing synergies would be observed at the VF-TH level, while not necessarily at the individual finger level. The results have only partially confirmed this hypothesis. Moment of force was stabilized at both VF-TH and IMRL levels during the steady-state phases, prior to and after the movement (PRE and POS). We would like to remind here that under stabilization we mean low variance across trials rather than mechanical or dynamic stability. During the movement, the moment-stabilizing synergy disappeared at both levels (see Figure 9 and 13). In contrast, the resultant normal and tangential forces were stabilized at the VF-TH level over the whole trial duration (see Figure 12A, B), while no such stabilization was seen at the IMRL level (see Figure 12C). The total tangential force applied to the handle was stabilized over the steady-state phases but not during the rotation (see Figure 12D). We will discuss implications of these findings for the interaction of synergies across the two hierarchical levels and different performance variables. However, first, we would like to address issues of the mechanics of rotation of a hand-held object.

The mechanics of quick rotation

In our experiment, the subject did not have to support the weight of the hand-held object, only to produce an accurate rotational action. This action involved a certain set of constraints. Consider only the grasp plane, which is a plane that contained all the sensor centers. The task of not producing a translational movement of the object implied that all the forces had to be perfectly balanced such that the resultant of both normal forces and tangential forces was close to zero. The moment of force in the grasp plane was supposed to be zero at the steady-states; it was expected to show a time profile similar to the object angular acceleration during the movement. The moment of force off the rotation plane was supposed to be zero at all movement phases.

The resultant force and resultant moment of force produced on the object got contributions from the same set of elemental variables (forces produced by individual digits). Hence, generating a time profile of the moment of force while avoiding changes in the resultant force was a non-trivial task, which likely required sequences of adjustments in elemental variables that may be described with chain effects (Zatsiorsky, Gao, & Latash, 2003b). Chain effects are sequences of cause-consequence pairs reflecting individual mechanical constraints that may lead to non-trivial correlations between pairs of elemental variables.

For example, in the initial position, the grip force (estimated as the thumb normal force in our study; note, however, that the resultant normal force was always very close to zero) was minimal because the weight of the handle was counter-balanced. During the movement, changes in the VF and TH tangential forces in opposite directions contributed to the moment of force (Figure 3). To avoid slippage, the subjects were forced to increase the normal forces in parallel with the tangential forces. Since the VF and TH normal forces were not perfectly collinear, they also contributed to the total moment of force.

The subjects showed a close to sigmoid angular trajectory with two peaks of M_{TOT} corresponding to the expected two-peaked acceleration typical of voluntary movements (Hogan, 1984; Mussa Ivaldi, Morasso, & Zaccaria, 1989). Peak values of M_{TOT} were higher during faster movements as could be expected from both basic mechanics and previous studies

NIH-PA Author Manuscript

NIH-PA Author Manuscript

NIH-PA Author Manuscript

(reviewed in Gottlieb, Corcos, & Agarwal, 1989). The main contributor to the M_{TOT} changes was the moment produced by the VF normal force. Note that the VF normal force had a relatively large range of possible lever arm changes reflected in its large center of pressure (COP) displacements (Figure 7). The index and little fingers were the main torque generators, similarly to findings in static tasks (Zatsiorsky et al., 2003b; Zatsiorsky et al., 2002). This result complies with the principle of mechanical advantage according to which force generators with larger lever arms produce larger shares of the total moment of force (Buchanan, Rovai, & Rymer, 1989; Prilutsky, 2000).

Grip force showed a low initial level expected based on the lack of external load. During the movement, F_{GRIP} showed an increase and, in seven out of the nine subjects, a reproducible time modulation with two peaks timed close to the peaks of M_{TOT} and a valley timed about M_{TOT}=0. These results support an idea that grip force adjustments during motion of a hand-held object happen in a feed-forward manner in anticipation of changes in the load that had to be counteracted by the tangential forces (Flanagan, Burstedt, & Johansson, 1999; Gao et al., 2005). The cited papers reported such F_{GRIP} adjustments to changes in the inertial load during linear movements of hand-held objects, while our study generalizes this conclusion for rotational movements associated with parallel changes in the moments of force produced by tangential and normal forces.

Antagonist moment production

When a person holds an object statically against a non-zero external load and a nonzero external torque, some fingers commonly produce moment of force acting not against the external torque but in the same direction. Such moments of force that apparently complicate the task for other fingers have been addressed as antagonist moments (Zatsiorsky et al., 2002). One of the explanations for the antagonist moments has been the phenomenon of enslaving, that is, unintended force production by fingers of a hand when other fingers produce force (Zatsiorsky, Li, & Latash, 2000). For example, if a person wants to produce a moment of force into supination with respect to an axis passing through a midpoint between the middle and ring fingers, purposeful normal force production by the little and ring fingers is required. Commands to these fingers, however, are expected to lead to unintended normal force production by the index and middle fingers that generate moments of force into pronation, i.e. antagonist moments.

In our experiments, antagonist moments (M_{ANT}) were seen at both hierarchical levels, VF-TH and IMRL. We used two indices to quantify moment of force production against the resultant M_{TOT}. At both levels, substantial antagonist moments were observed with significant effects of the hand position at steady-states and a drop in the co-contraction indices during the movement. The dependence of antagonist moment magnitude at the IMRL level on wrist position suggests that enslaving effects among the fingers may be position dependent, an insight in line with a recent study by Kim and colleagues (Kim, Shim, Zatsiorsky, & Latash, 2008). The modulation of M_{ANT} produced by the thumb (at the TH-VF level) with wrist position was opposite to that seen at the IMRL level. Namely, the thumb produced higher M_{ANT} at PR while the fingers produced higher M_{ANT} at SU. It is possible that the unavoidable differences in M_{ANT} produced by the fingers due to the enslaving effects were partly compensated by the opposite differences in M_{ANT} produced by the thumb.

In some papers, the production of antagonist moments has been associated with a particular neural strategy of increasing the rotational wrist apparent stiffness; in particular, elderly show increased antagonist moments (Shim, Lay, Zatsiorsky, & Latash, 2004) possibly related to their decreased ability to produce desired rotational hand actions (Olafsdottir, Zhang, Zatsiorsky, & Latash, 2007). On the other hand, fast movements have been associated with a transient increase in the joint apparent stiffness (Latash & Zatsiorsky, 1993; Latash & Gottlieb, 1991). Hence,

NIH-PA Author Manuscript

NIH-PA Author Manuscript

NIH-PA Author Manuscript

our finding of a drop in the antagonist moments during the fast movement speaks against an idea that these moments contribute to the apparent stiffness of the multi-digit system that produced the handle rotation.

Synergies at the two hierarchical levels

The presence of a two-level hierarchy by itself favors competition between synergies at the two levels. Indeed, synergies are associated with relatively more "good variance" (that does not affect performance) as compared to "bad variance" (that does) (reviewed in Latash et al., 2007). Hence, a synergy stabilizing the overall output of the system may be expected to be accompanied by considerable "good variance" at the higher level of the hierarchy, which may be beneficial for performing secondary tasks or dealing with possible external perturbations (Zhang, Scholz, Zatsiorsky, & Latash, 2008). The large "good variance" component translates into proportionally large variance of each of the elements, for example VF. However, when considered at the lower level of the hierarchy, VF variance is "bad" by definition, and having a large value of this variance component makes it difficult for the controller to organize a synergy at the lower level (Gorniak et al., 2007b).

Some of the findings (summarized in Table 3) support this logic. In particular, the resultant normal force was stabilized at the VF-TH level by co-varied changes in the normal forces produced by the TH and VF at all phases of the movement. In contrast, at the lower, IMRL level, the total normal force produced by the VF was not stabilized (Figure 12). These results are similar to those reported earlier (Gorniak et al., 2007a,b).

However, other variables could show deviations from this predicted pattern (Table 3). In particular, at steady-states, the moments produced by the VF and TH forces co-varied negatively thus stabilizing the total moment produced on the handle. The same was true for the VF moment of force stabilized by the co-varied changes in the moments of force produced by individual fingers. During the movement, the synergy index ΔV became negative at both levels signifying loss of moment-stabilizing synergies.

The resultant tangential force was stabilized at the VF-TH level at all movement phases; while at the IMRL level; the VF tangential force was stabilized at steady-states but not during the movement.

Two conclusions can be drawn from these findings. First, a quick change in a variable is less likely to be associated with its stabilization. In particular, moment-stabilizing synergies were lost at both hierarchical levels, while tangential force-stabilizing synergies were lost at the IMRL level during the handle rotation. These observations are similar to earlier reports of weakened or lost synergies during fast force production (Latash, Scholz, Danion, & Schoner, 2002c; Olafsdottir, Yoshida, Zatsiorsky, & Latash, 2005; Shim, Olafsdottir, Zatsiorsky, & Latash, 2005c). One interpretation of these results is that the controller may turn off synergies if a quick change in related variables is required. This conclusion has been supported by changes in synergy indices in anticipation of a quick action, so-called anticipatory synergy adjustments (Kim, Shim, Zatsiorsky, & Latash, 2006; Olafsdottir et al., 2005; Shim, Park, Zatsiorsky, & Latash, 2006). An alternative explanation is based on an assumption that the CNS is able to ensure co-variation of the magnitudes of elemental variables but not of their timing parameters (Latash et al., 2002c). Then, an increase in the rate of change of a performance variable during the movement is expected to be associated with an increase in its variability and a corresponding drop in the synergy index. However, this explanation implies that a stronger drop in the synergy index is expected during fast movements as compared to slow movements, a prediction not supported by the results (Figures 11 and 12).

NIH-PA Author Manuscript

NIH-PA Author Manuscript

NIH-PA Author Manuscript

The second conclusion is that the relations between synergies at the two hierarchical levels are not as straightforward as suggested earlier. Obviously, the controller is able to organize synergies stabilizing a performance variable at both levels, although only at steady-states. Some of these patterns may be interpreted based on the explicit and implicit task constraints. For example, the task of not producing any translational movement of the handle required very small values of both normal and tangential total force and very small variability of those values across trials. Hence, a synergy stabilizing those forces at the TH-VF level looks like a very desirable mechanism. Note, however, that it is not obligatory because a low level of variability of either of those variables could have been achieved with comparably low "bad variability" and "good variability" resulting in non-positive ΔV values. The same is true with respect to the total moment at steady-states. However, during the movement M_{TOT} changed quickly, and these changes could show substantial trial-to-trial variability ("bad variability") resulting in a loss of the moment stabilizing synergy.

The different patterns of synergies for the total force and total moment of force may be viewed as providing further support for the principle of superposition in human prehension (Arimoto, Tahara, Yamaguchi, Nguyen, & Han, 2001; Zatsiorsky, Latash, Gao, & Shim, 2004). According to this principle, control of a complex action, such as prehension, may benefit from having several controllers dedicated to action components. The original studies (Arimoto et al., 2001) have shown that such a design saves computation time for the control of robotic hands. Later, studies of human static prehension have confirmed that the grasping action and the rotational action may be based on separate groups of elemental variables that show strong co-variation across trials within a group but not between groups (Shim et al., 2003, 2005b). Our results suggest that the principle of superposition may not be limited to static tasks but represents a general principle of the organization of prehensile actions.

Concluding Comments

This is the first study to perform a detailed mechanical analysis of the multi-digit action during accurate rotational tasks involving all five digits of the human hand. The study has confirmed applicability of some of the known principles, such as the principle of mechanical advantage and the principle of superposition, formulated earlier based on experiments with more constrained tasks, to more natural tasks. It has also shown that the trade-off between synergies at different levels of a control hierarchy can be handled by the central nervous system in a much more subtle and versatile way as compared to the patterns observed in more constrained tasks. Results of this study may be used to explore causes of hand function impairments in a variety of conditions including healthy aging (cf. Olafsdottir et al. 2007).

Acknowledgments

The study was in part supported by NIH grants AG-018751, NS-035032, AR-048563, and M01 RR-10732.

References

Arbib, MA.; Iberall, T.; Lyons, D. Coordinated control programs for movements of the hand. In: Goodwin, AW.; Darian-Smith, I., editors. Hand function and the neocortex. Berlin: Springer-Verlag; 1985. p. 111-129.

Arimoto S, Nguyen PT, Han HY, Doulgeri Z. Dynamics and control of a set of dual fingers with soft tips. Robotica 2000;18:71–80.

Arimoto S, Tahara K, Yamaguchi M, Nguyen PTA, Han HY. Principles of superposition for controlling pinch motions by means of robot fingers with soft tips. Robotica 2001;19:21–28.

Baud-Bovy G, Soechting JF. Two virtual fingers in the control of the tripod grasp. Journal of Neurophysiology 2001;86:604–615. [PubMed: 11495936]

Bernstein, NA. The co-ordination and regulation of movements. Oxford: Pergamon Press; 1967.

NIH-PA Author Manuscript

NIH-PA Author Manuscript

NIH-PA Author Manuscript

Bernstein, NA. On dexterity and its development. In: Latash, ML.; Turvey, MT., editors. Dexterity and its development. Erlbaum: Mahwah; 1996.

Bernstein, NA. On the construction of movements. Moscow: Medgiz; 1947.

Buchanan TS, Rovai GP, Rymer WZ. Strategies for muscle activation during isometric torque generation at the human elbow. Journal of Neurophysiology 1989;62:1201–1212. [PubMed: 2600619]

Bursztyn LL, Flanagan JR. Sensorimotor memory of weight asymmetry in object manipulation. Experimental Brain Research 2008;184:127–133.

Cutkosky, MR.; Howe, RD. Dexterous robot hands. New York: Springer-Verlag; 1990.

Flanagan JR, Burstedt MK, Johansson RS. Control of fingertip forces in multidigit manipulation. Journal of Neurophysiology 1999;81:1706–1717. [PubMed: 10200206]

Gao F, Latash ML, Zatsiorsky VM. Internal forces during object manipulation. Experimental Brain Research 2005;165:69–83.

Gorniak SL, Zatsiorsky VM, Latash ML. Emerging and disappearing synergies in a hierarchically controlled system. Experimental Brain Research 2007a;183:259–270.

Gorniak SL, Zatsiorsky VM, Latash ML. Hierarchies of synergies: an example of two-hand, multi-finger tasks. Experimental Brain Research 2007b;179:167–180.

Gottlieb GL, Corcos DM, Agarwal GC. Organizing principles for single-joint movements. I. A speed-insensitive strategy. Journal of Neurophysiology 1989;62:342–357. [PubMed: 2769334]

Hogan N. An organizing principle for a class of voluntary movements. Journal of Neuroscience 1984;4:2745–2754. [PubMed: 6502203]

Kang N, Shinohara M, Zatsiorsky VM, Latash ML. Learning multi-finger synergies: an uncontrolled manifold analysis. Experimental Brain Research 2004;157:336–350.

Kim SW, Shim JK, Zatsiorsky VM, Latash ML. Anticipatory adjustments of multi-finger synergies in preparation for self-triggered perturbations. Experimental Brain Research 2006;174:604–612.

Kim SW, Shim JK, Zatsiorsky VM, Latash ML. Finger inter-dependence: Linking the kinetic and kinematic variables. Human Movement Science 2008;27:408–422. [PubMed: 18255182]

Latash ML, Gottlieb GL. Reconstruction of shifting elbow joint compliant characteristics during fast and slow movements. Neuroscience 1991;43:697–712. [PubMed: 1922790]

Latash ML, Kang N, Patterson D. Finger coordination in persons with Down syndrome: atypical patterns of coordination and the effects of practice. Experimental Brain Research 2002a;146:345–355.

Latash ML, Li S, Danion F, Zatsiorsky VM. Central mechanisms of finger interaction during one- and two-hand force production at distal and proximal phalanges. Brain Research 2002b;924:198–208. [PubMed: 11750905]

Latash ML, Scholz JF, Danion F, Schoner G. Finger coordination during discrete and oscillatory force production tasks. Experimental Brain Research 2002c;146:419–432.

Latash ML, Scholz JP, Schoner G. Toward a new theory of motor synergies. Motor Control 2007;11:276–308. [PubMed: 17715460]

Latash ML, Zatsiorsky VM. Joint stiffness: myth or reality? Human Movement Science 1993;12:653–692.

Mackenzie, CL.; Iberall, T. The grasping hand. North-Holland: Amsterdam; 1994.

Mason, MT.; Salisbury, KJ., editors. Robot hands and the mechanics of manipulation (artificial intelligence). Cambridge, MA: MIT press; 1985.

Mussa Ivaldi FA, Morasso P, Zaccaria R. Kinematic neetworks. A distributed model for representing and regularizing motor redundancy. Biological Cybernetics 1989;60:1–16. [PubMed: 3214648]

Olafsdottir H, Yoshida N, Zatsiorsky VM, Latash ML. Anticipatory covariation of finger forces during self-paced and reaction time force production. Neuroscience Letters 2005;381:92–96. [PubMed: 15882796]

Olafsdottir H, Zhang W, Zatsiorsky VM, Latash ML. Age-related changes in multifinger synergies in accurate moment of force production tasks. Journal of Applied Physiology 2007;102:1490–1501. [PubMed: 17204576]

Pataky TC, Latash ML, Zatsiorsky VM. Prehension synergies during nonvertical grasping, I: Experimental observations. Biological Cybernetics 2004a;91:148–158. [PubMed: 15378373]

NIH-PA Author Manuscript

NIH-PA Author Manuscript

NIH-PA Author Manuscript

Pataky TC, Latash ML, Zatsiorsky VM. Prehension synergies during nonvertical grasping, II: Modeling and optimization. Biological Cybernetics 2004b;91:231–242. [PubMed: 15503126]

Prilutsky BI. Coordination of two- and one-joint muscles: functional consequences and implications for motor control. Motor Control 2000;4:1–44. [PubMed: 10675807]

Santello M, Soechting JF. Force synergies for multifingered grasping. Experimental Brain Research 2000;133:457–467.

Scholz JP, Kang N, Patterson D, Latash ML. Uncontrolled manifold analysis of single trials during multi-finger force production by persons with and without Down syndrome. Experimental Brain Research 2003;153:45–58.

Shim JK, Latash ML, Zatsiorsky VM. Finger coordination during moment production on a mechanically fixed object. Experimental Brain Research 2004;157:457–467.

Shim JK, Latash ML, Zatsiorsky VM. Prehension synergies in three dimensions. Journal of Neurophysiology 2005a;93:766–776. [PubMed: 15456799]

Shim JK, Latash ML, Zatsiorsky VM. Prehension synergies: trial-to-trial variability and hierarchical organization of stable performance. Experimental Brain Research 2003;152:173–184.

Shim JK, Latash ML, Zatsiorsky VM. Prehension synergies: trial-to-trial variability and principle of superposition during static prehension in three dimensions. Journal of Neurophysiology 2005b; 93:3649–3658. [PubMed: 15728759]

Shim JK, Lay BS, Zatsiorsky VM, Latash ML. Age-related changes in finger coordination in static prehension tasks. Journal of Applied Physiology 2004;97:213–224. [PubMed: 15003998]

Shim JK, Olafsdottir H, Zatsiorsky VM, Latash ML. The emergence and disappearance of multi-digit synergies during force-production tasks. Experimental Brain Research 2005c;164:260–270.

Shim JK, Park J, Zatsiorsky VM, Latash ML. Adjustments of prehension synergies in response to self-triggered and experimenter-triggered load and torque perturbations. Experimental Brain Research 2006;175:641–653.

Winges SA, Eonta SE, Soechting JF, Flanders M. Multi-digit control of contact forces during rotation of a hand-held object. Journal of Neurophysiology 2008;99:1846–1856. [PubMed: 18234979]

Zatsiorsky, VM. Kinetics of human motion. Champaign, IL: Human Kinetics; 2002.

Zatsiorsky VM, Gao F, Latash ML. Finger force vectors in multi-finger prehension. Journal of Biomechanics 2003a;36:1745–1749. [PubMed: 14522218]

Zatsiorsky VM, Gao F, Latash ML. Prehension synergies: effects of object geometry and prescribed torques. Experimental Brain Research 2003b;148(1):77–87.

Zatsiorsky VM, Gregory RW, Latash ML. Force and torque production in static multifinger prehension: biomechanics and control. I. Biomechanics. Biological Cybernetics 2002;87:50–57. [PubMed: 12111268]

Zatsiorsky VM, Latash M, Gao F, Shim JK. The principle of superposition in human prehension. Robotica 2004;22:231–234.

Zatsiorsky VM, Latash ML. Prehension synergies. Exercise and Sport Science Reviews 2004;32:75–80.

Zatsiorsky VM, Li ZM, Latash ML. Enslaving effects in multi-finger force production. Experimental Brain Research 2000;131:187–195.

Zhang W, Scholz JP, Zatsiorsky VM, Latash ML. What do synergies do? Effects of secondary constraints on multidigit synergies in accurate force-production tasks. Journal of Neurophysiology 2008;99:500–513. [PubMed: 18046000]

NIH-PA Author Manuscript
NIH-PA Author Manuscript
NIH-PA Author Manuscript

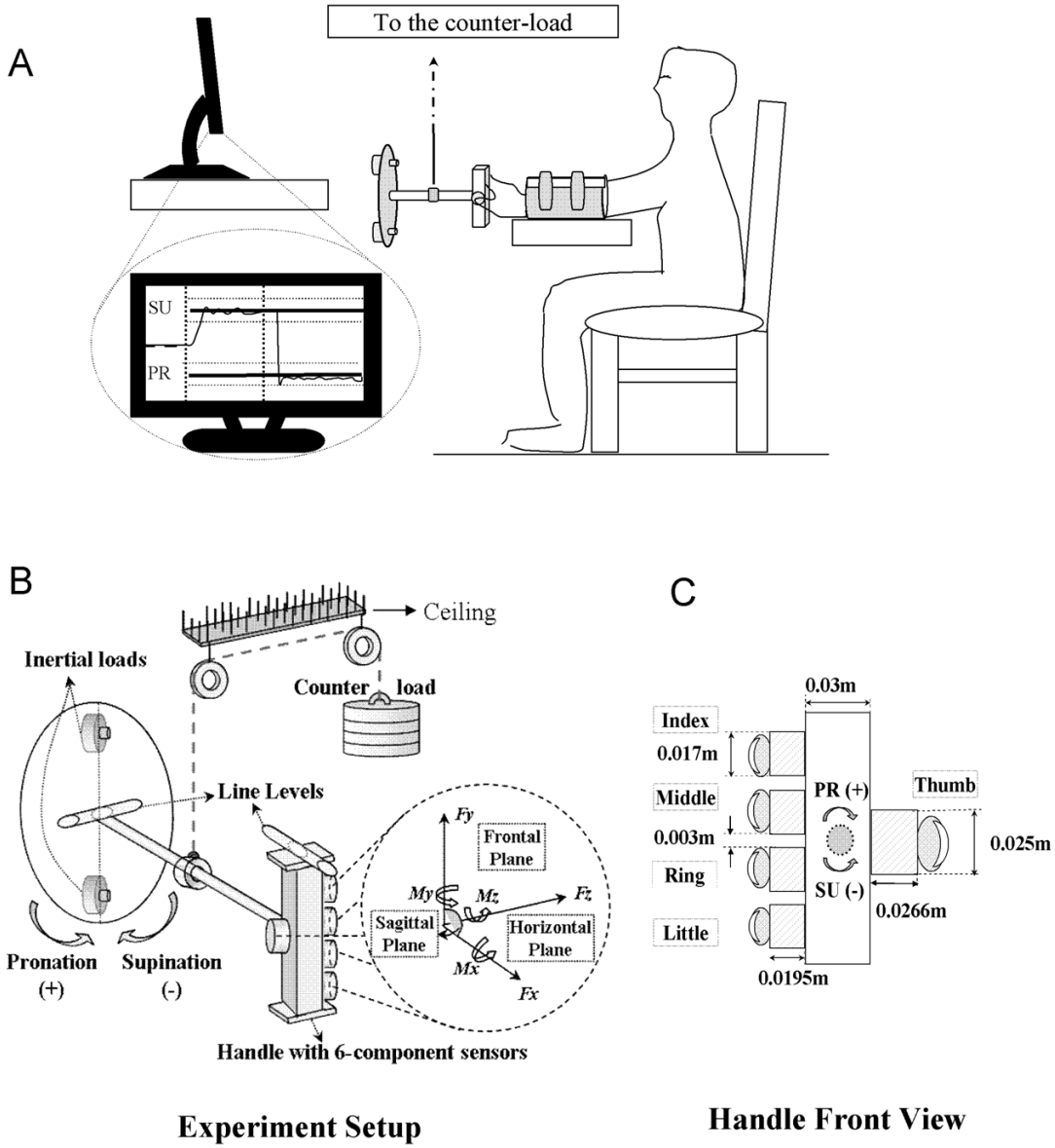

Figure 1.
Experimental set up. A: The subject and arm positions; B: The disk, rod and handle (DRH) system with the counter-load; and C: The vertical handle with the six-component force/torque sensors.

NIH-PA Author Manuscript

NIH-PA Author Manuscript

NIH-PA Author Manuscript

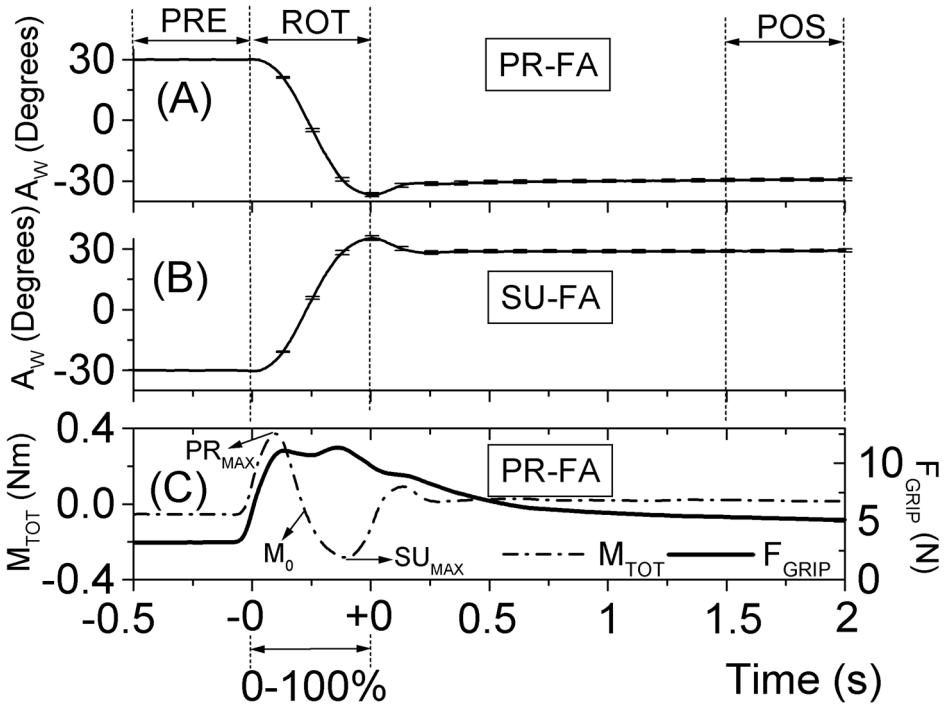

Figure 2.

A and B: Time profiles of the rotation angle (A_W) with standard errors computed across trials for a typical subject during fast movements (FA) from supination to pronation (PR; panel A) and from pronation to supination (SU; panel B). PRE refers to a 0.5-s interval prior to the movement initiation; ROT refers to the rotation interval; POS refers to a 0.5-s duration 1.5 s after the movement termination. C: Time profiles of the resultant moment of force (M_{TOT}; dash-dot line) and grip force (normal force of the thumb, F_{GRIP}; solid line) for the PR-FA condition. The time point when peak pronation (PR_{MAX}), peak supination (SU_{MAX}) and M_{TOT} transient to zero (M_0) during the movement are shown by arrows. The initiation and termination of the movement are shown as negative (−0) and positive (+0) zero respectively. The movement cycle was normalized into 100%. Time duration before and after movement are in seconds.

NIH-PA Author Manuscript

NIH-PA Author Manuscript

NIH-PA Author Manuscript

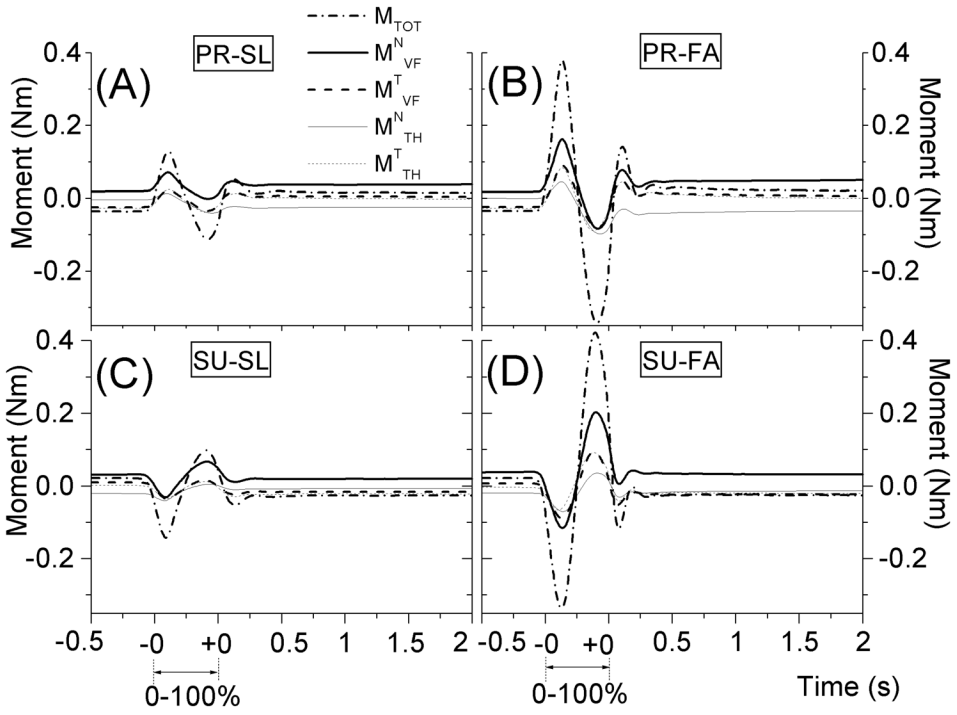

Figure 3.

Time profiles of the resultant moment of force (M_{TOT}; thick dash-dot lines) and its four components produced by the normal and tangential forces of the virtual finger (M^N_{VF}, thick solid lines; M^T_{VF}, thick dashed lines) and thumb (M^N_{TH}, thin solid lines; M^T_{TH}, thin dashed lines) averaged across subjects under the four conditions. A: Slow, from supination to pronation (PR-SL). B: Fast, from supination to pronation (PR-FA). C: Slow, from pronation to supination (SU-SL). D: Fast, from pronation to supination (SU-FA). For other abbreviations see Figure 2.

NIH-PA Author Manuscript

NIH-PA Author Manuscript

NIH-PA Author Manuscript

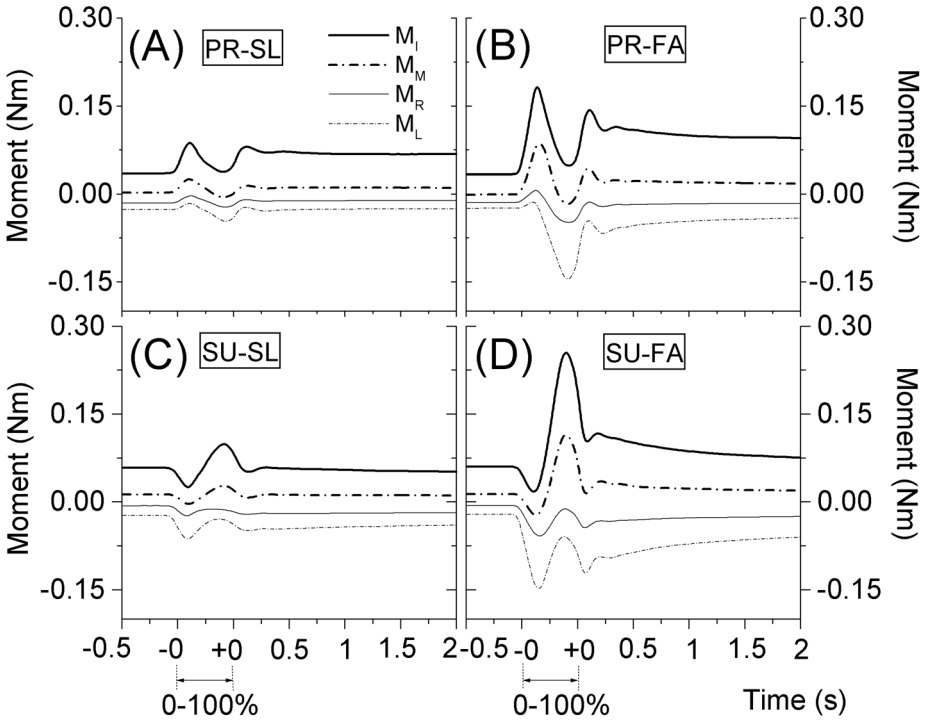

Figure 4.

Time profiles of moments produced by index (M_I; thick solid line), middle (M_M; thick dashed-dotted line), ring (M_R; thin solid line) and little (M_L; thin dashed-dotted line) finger averaged across subjects under four conditions: A: PR-SL; B: PR-FA; C: SU-SL; D: SU-FA. For abbreviations see Figures 2 and 3.

NIH-PA Author Manuscript
NIH-PA Author Manuscript
NIH-PA Author Manuscript

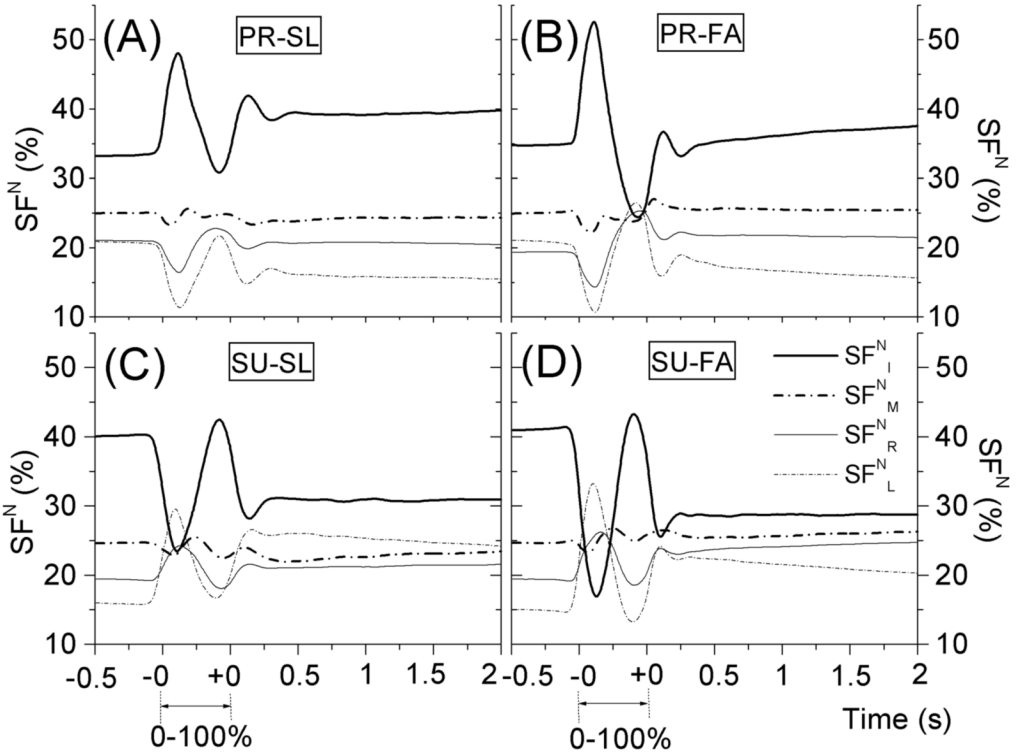

Figure 5.

Time profiles of the sharing indices of the normal force (F^N in percent) for the index (SF^N_I; thick solid line), middle (SF^N_M; thick dash-dot line), ring (SF^N_R; thin solid line) and little (SF^N_L; thin dash-dot line) finger averaged across subjects under four conditions: A: PR-SL; B: PR-FA; C: SU-SL; D: SU-FA. For abbreviations see Figures 2 and 3.

NIH-PA Author Manuscript

NIH-PA Author Manuscript

NIH-PA Author Manuscript

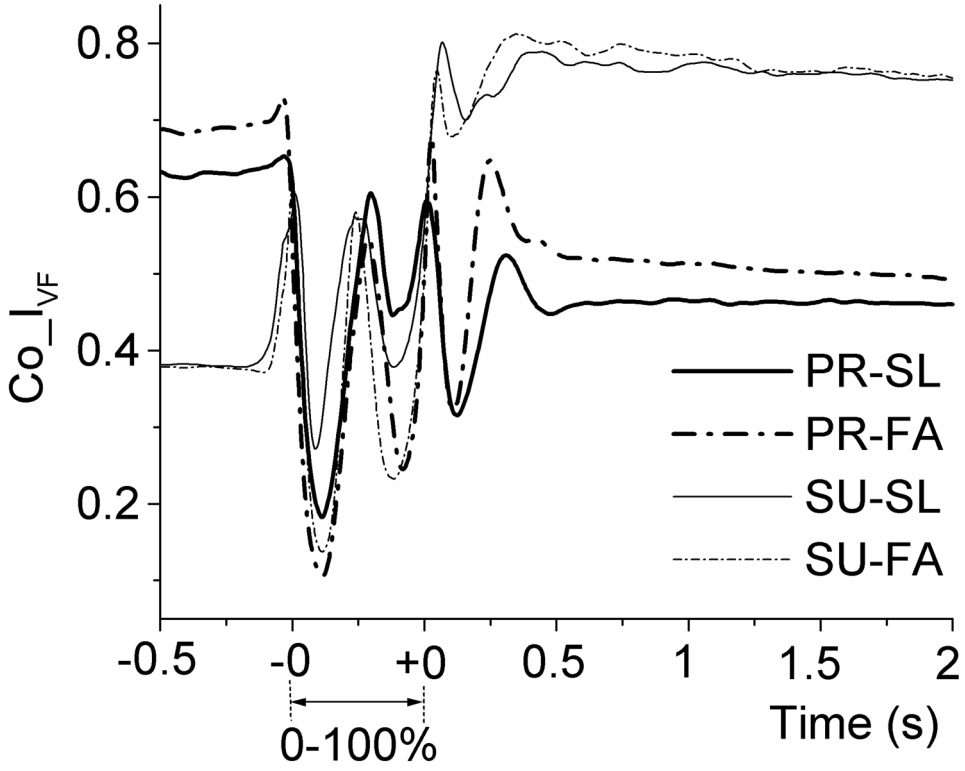

Figure 6.
Time profiles of the co-contraction index (Co_I_{VF}) averaged across subjects under the four conditions: PR-SL in thick solid line; PR-FA in thick dashed-dotted line; SU-SL in thin solid line; SU-FA in thin dashed-dotted line. Y axis is unitless. For abbreviations see Figures 2 and 3.

NIH-PA Author Manuscript

NIH-PA Author Manuscript

NIH-PA Author Manuscript

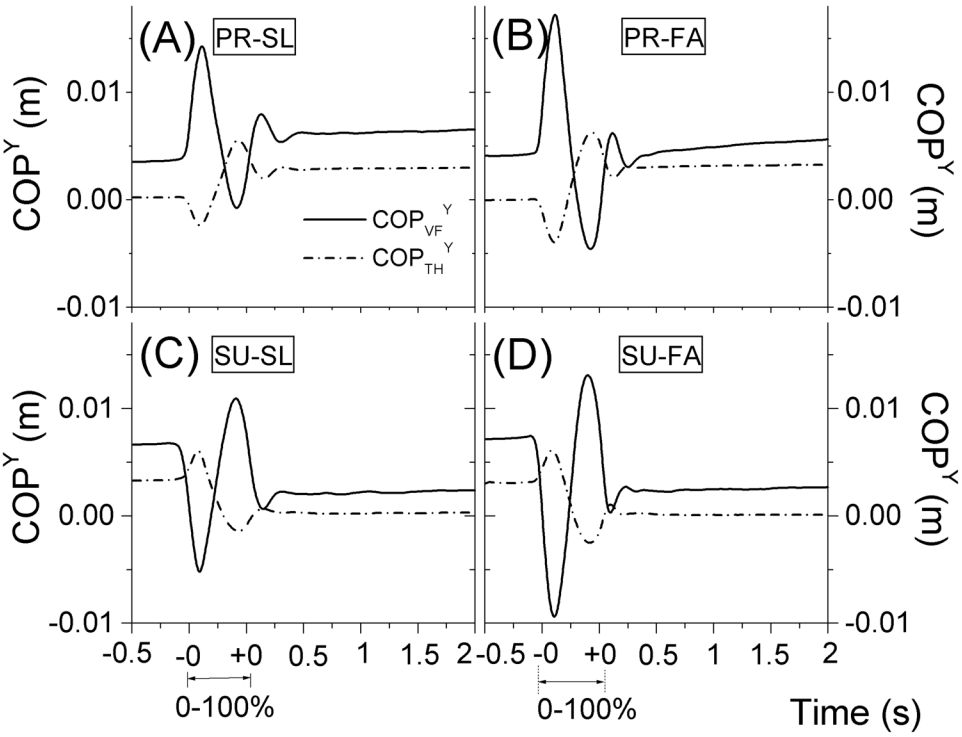

Figure 7.
Time profiles of the center of pressure (COP_Y) of the normal force of virtual finger (COP_{VF}^Y; thick solid line) and of the thumb (COP_{TH}^Y, thick dashed-dotted line) averaged across subjects under the four conditions: A: PR-SL; B: PR-FA; C: SU-SL; D: SU-FA. For abbreviations see Figures 2 and 3.

NIH-PA Author Manuscript

NIH-PA Author Manuscript

NIH-PA Author Manuscript

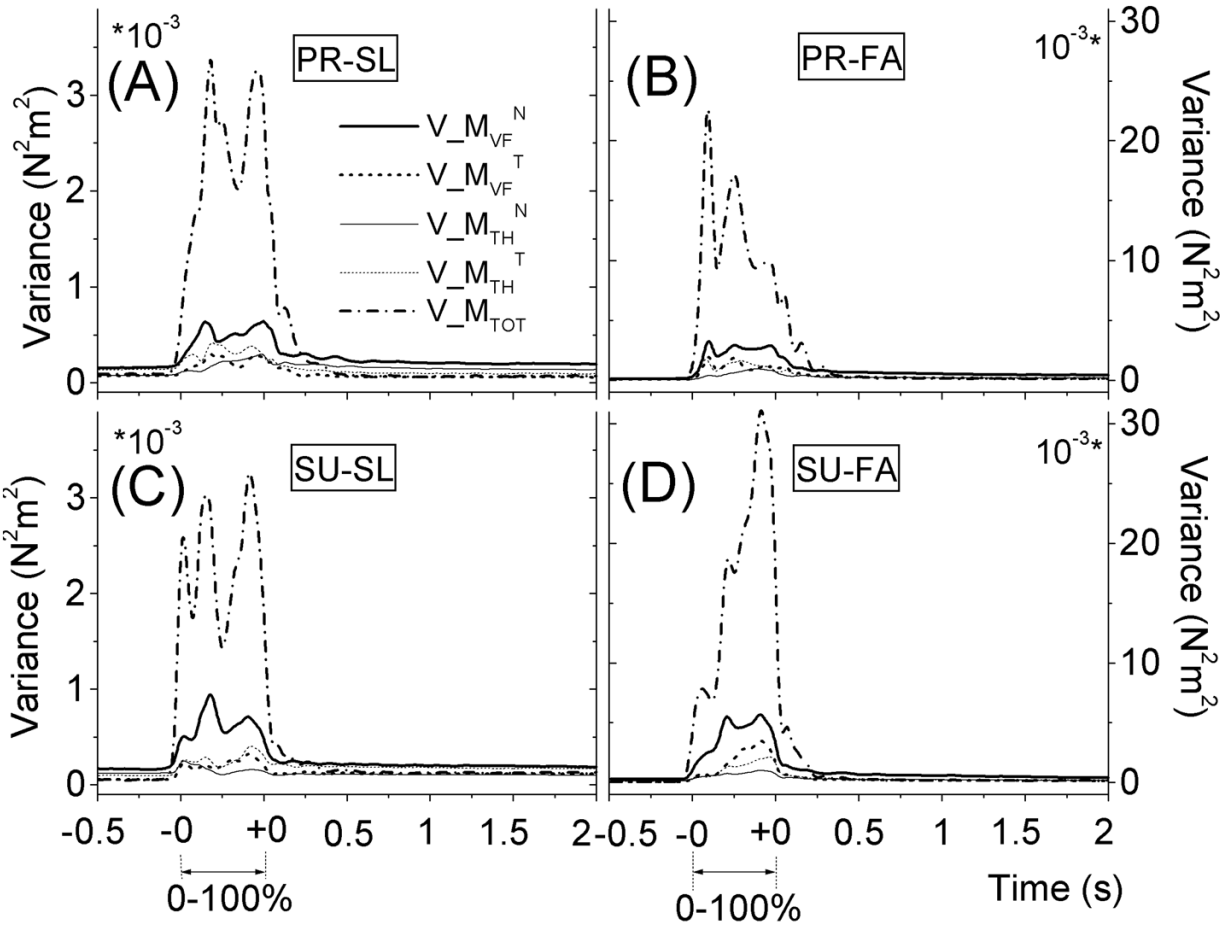

Figure 8.

Time profiles of the variance of the resultant moment (V_MTOT) and variances of four moment components at VF-TH level produced by normal force of virtual finger ($V\_M_{VF}^{N}$; thick solid line), tangential force of virtual finger ($V\_M_{VF}^{T}$; thick dashed line), normal force of thumb ($V\_M_{TH}^{N}$; thin solid line) and tangential force of thumb (V_{TH}^{T}; thin dashed line) averaged across subjects under four conditions: A: PR-SL; B: PR-FA; C: SU-SL; D: SU-FA. For abbreviations see Figures 2 and 3.

NIH-PA Author Manuscript

NIH-PA Author Manuscript

NIH-PA Author Manuscript

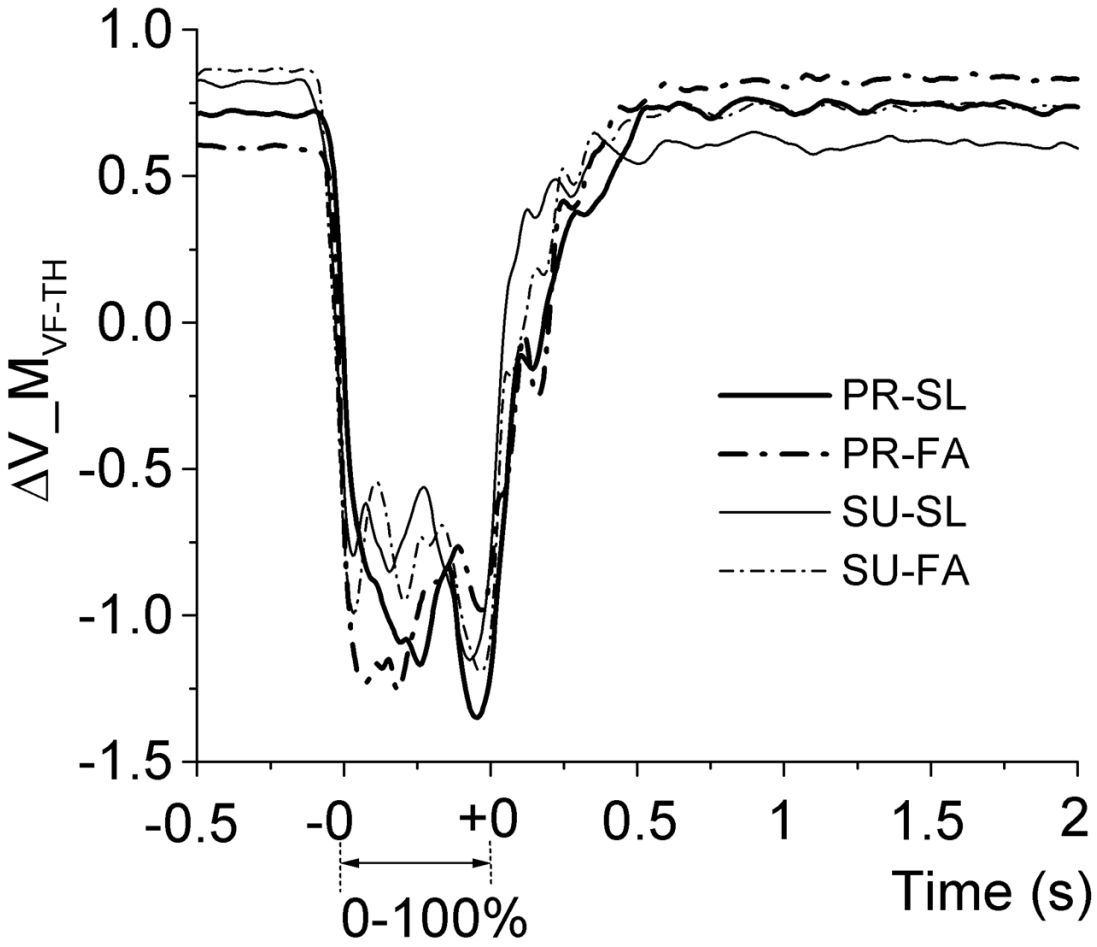

Figure 9.

Time profiles of ΔV indices for the resultant moment (ΔV_M_{VF-TH}) at the VF-TH level averaged across subjects under the four conditions: PR-SL in thick solid line; PR-FA in thick dashed-dotted line; SU-SL in thin solid line; SU-FA in thin dashed-dotted line. For abbreviations see Figures 2 and 3.

NIH-PA Author Manuscript

NIH-PA Author Manuscript

NIH-PA Author Manuscript

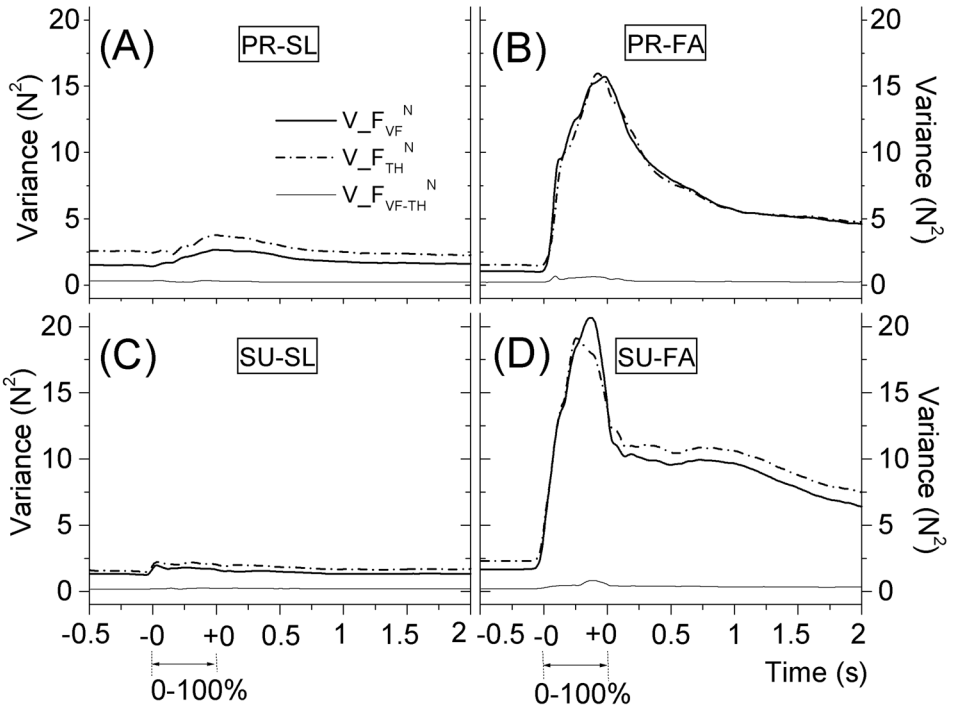

Figure 10.

Time profiles of the variances of resultant normal force ($V\_F_{VF+TH}^{N}$; thin solid line), of the VF normal force ($V\_F_{VF}^{N}$; thick solid line), and of the thumb normal force ($V\_F_{TH}^{N}$; thick dashed-dotted line) averaged across subjects under the four conditions: A: PR-SL; B: PR-FA; C: SU-SL; D: SU-FA. For abbreviations see Figures 2 and 3.

NIH-PA Author Manuscript

NIH-PA Author Manuscript

NIH-PA Author Manuscript

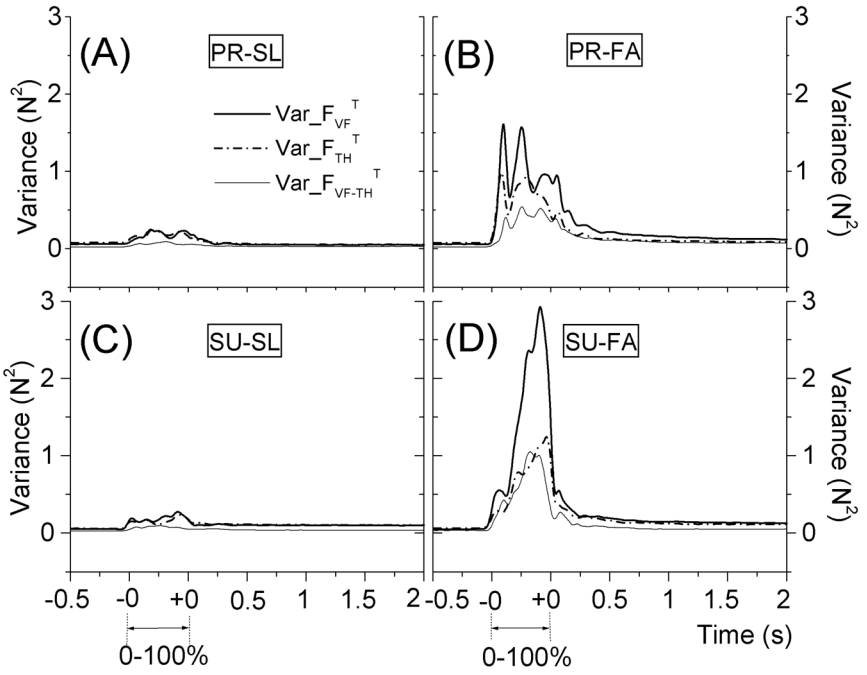

Figure 11.

Time profiles of the variances of resultant tangential force ($V\_F_{VF+TH}{}^{T}$; thin solid line), of the VF tangential force ($V\_F_{VF}{}^{T}$; thick solid line), and of the thumb tangential force ($V\_F_{TH}{}^{T}$; thick dashed-dotted line) averaged across subjects under the four conditions: A): PR-SL; B): PR-FA; C): SU-SL; D): SU-FA. For abbreviations see Figures 2 and 3.

NIH-PA Author Manuscript
NIH-PA Author Manuscript
NIH-PA Author Manuscript

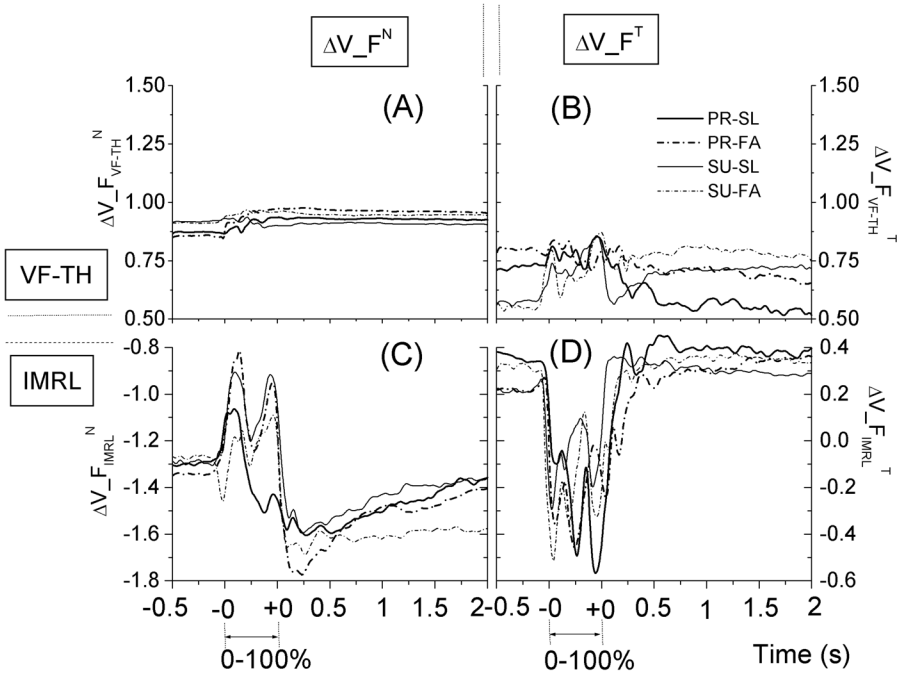

Figure 12.

Time profiles of ΔV for the resultant normal force at the VF-TH level ($\Delta V\_F_{VF-TH}^{N}$; panel A), resultant tangential force at the VF-TH level ($\Delta V\_F_{VF-TH}^{T}$; panel B), VF normal force at the IMRL level ($\Delta V\_F_{IMRL}^{N}$; panel C), and VF tangential force at the IMRL level ($\Delta V\_F_{IMRL}^{T}$; panel D) averaged across subjects under the four conditions: PR-SL in thick solid line; PR-FA in thick dashed-dotted line; SU-SL in thin solid line; SU-FA in thin dashed-dotted line. For abbreviations see Figures 2 and 3.

NIH-PA Author Manuscript

NIH-PA Author Manuscript

NIH-PA Author Manuscript

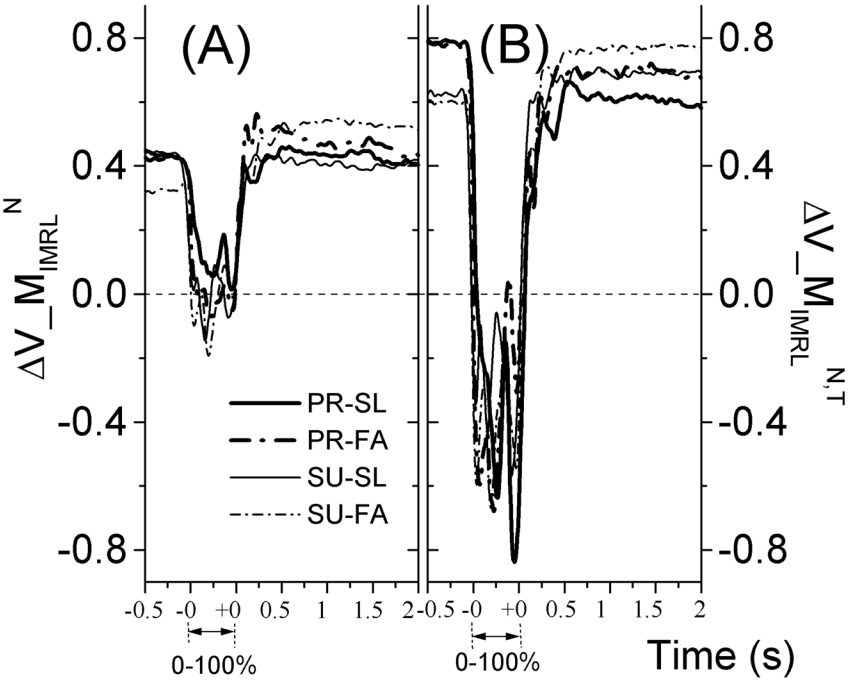

Figure 13.

Time profiles of ΔV indices for the VF moment of normal force ($\Delta V\_M_{IMRL}^{N}$; panel A) and VF moment of total force ($\Delta V\_M_{IMRL}^{N,T}$; panel B) at the IMRL level averaged across subjects under the four conditions: PR-SL in thick solid line; PR-FA in thick dashed-dotted line; SU-SL in thin solid line; SU-FA in thin dashed-dotted line. For abbreviations see Figures 2 and 3.

NIH-PA Author Manuscript
NIH-PA Author Manuscript
NIH-PA Author Manuscript

Table 1

Average performance variables

			PR-SL	PR-FA	SU-SL	SU-FA
Amplitude of A_W (deg)			60.4±0.4	63.9±0.9	61±0.4	63.4±0.5
Time of ROT (s)			0.44±0.04	0.29±0.03	0.41±0.03	0.28±0.03
M_{TOT} (Nm)	PR_{MAX}		0.145±0.024	0.428±0.129	0.125±0.021	0.455±0.121
	SU_{MAX}		−0.133±0.024	−0.365±0.079	−0.162±0.022	−0.381±0.062
F_{GRIP} (N)	PRE		5.9±1.1	5.1±0.7	4.9±1	5.1±1.1
	POS		6.1±1.6	9.8±1.6	7.2±1.3	11.6±3.2
	ROT	T_PR_{MAX}	6.9±1.4	12.1±2.3	7.8±1.4	19.8±4.7
		T_SU_{MAX}	6.7±1.8	16.5±3.9	6.3±1.2	12.7±2.2
		T_M_0	6.2±1.7	14.1±2.6	6.8±1.4	16.8±3.8

Mean data across subjects are shown with standard errors. PR-SL: pronation, slow; PR-FA: pronation, fast; SU-SL: supination, slow; SU-FA: supination, fast; A_W: the pronation-supination angle; ROT: the rotational action; PRE: the time interval before the action; POS –the time interval after the action; M_{TOT}: total moment of force represented by two indices, PR_{MAX} and SU_{MAX} (peak values into pronation and supination, respectively). PR_{MAX}: maximal value of M_{TOT} in pronation; SU_{MAX}: maximal value of M_{TOT} in supination; F_{GRIP}: the normal force of the thumb, which is reported for different time intervals (PRE, POS, and ROT) and instants (T_PR_{MAX}, T_SU_{MAX} and T_M_0); T_PR_{MAX}: time of PR_{MAX}; T_SU_{MAX}: time of SU_{MAX}; T_M_0: time when M_{TOT} = 0.

NIH-PA Author Manuscript
NIH-PA Author Manuscript
NIH-PA Author Manuscript

Table 2

Average co-contraction (Co_I_{TH}) index for thumb.

		PR-SL	PR-FA	SU-SL	SU-FA
Co_I_{TH}	ROT	17.6±3.9	10.1±2.7	18.3±3.3	9.1±2
	PRE	13±9.3	7.6±4.2	82.5±5.7	66.4±9.8
	POS	68.7±12.9	79.8±5.7	17.6±11.5	12.4±7.7

Co_I_{TH}: the co-contraction index calculated for the thumb for different time intervals. Average data across subjects are presented with standard errors. For other abbreviations see Table 1.

NIH-PA Author Manuscript

NIH-PA Author Manuscript

NIH-PA Author Manuscript

Table 3

Summary of the synergy analysis

		ΔV		
		M	**F^N**	**F^T**
VF-TH level	Steady states phases	>0	>0	>0
	Movement phase	<0	>0	>0
IMRL level	Steady states phases	>0	<0	>0
	Movement phase	<=0	<0	<0

VF-TH: virtual finger – thumb level; IMRL: individual finger level; ΔV: the index of synergy; ΔV>0 means a synergy stabilizing the variable (M, F^N, or F^T) at the selected level of analysis (VF-TH or IMRL), ΔV≤0 indicates no synergy stabilizing the variable at the selected level. M: resultant moment of force; F^N: normal force; F^T: tangential force.